RESERVOIR ENGINEERING STUDY OF THE KRAFLA-HVITHOLAR GEOTHERMAL AREA, ICELAND.

Abatneh Wale*
UNU Geothermal Training Programme,
National Energy Authority (NEA),
Grensasvegur 9, 108 Reykjavik,
ICELAND.

*Permanent address:
Geothermal Energy Exploration Project,
Geological Survey of Ethiopia,
Ministry of Mines and Energy,
P.O. Box 2302, Addis Ababa,
ETHIOPIA.

ABSTRACT

At present the Krafla geothermal power plant in Iceland utilizes three production fields. These are the Leirbotnar area, the southern slopes of Mt. Krafla and the Hvitholar areas.

The results of a reservoir engineering study of the Krafla-Hvitholar geothermal area are presented. Injection, fall-off, pressure recovery, temperature logs, pressure logs and discharge measurements data are used for this study. Pressure transient data is interpreted using the semilog method, type curve matching, and Jacob's and Rorabaugh's method. The results indicate a transmissivity of $1.3\text{-}1.9\times10^{-7}$ $m^3/P_a\cdot s$ for well KJ-21, a value of $2\text{-}6\times10^{-8}$ $m^3/P_a\cdot s$ for well KJ-22 and a value of $0.8\times10^{-8} m^3/P_a\cdot s$ for well KJ-23. The transmissivity value estimated for well KJ-21 on the basis of a 3 month pressure recovery is in a good agreement with the value estimated on the basis of the injection test.

Temperature and pressure logs clearly illustrate potential feed points and cross flow between aquifers. The general temperature profile in the area is characterized by a temperature reversal, having a maximum temperature of 260°C around 600 m depth.

TABLE OF CONTENTS

LIST OF FIGURES

LIST OF TABLES

LIST OF SYMBOLS

P	pressure, Pa
r	radial distance, m
ϕ	porosity, fraction
μ	dynamic viscosity, Pa.s
C_t	total compressibility, Pa^{-1}
P_D	dimensionless pressure
t_D	dimensionless time
t	time, s
r_D	dimensionless radial distance, (r/r_w)
r_w	radius of wellbore, m
P_i	initial pressure, Pa
h	aquifer thickness, m
E_i	exponential integral
q	flow rate, m3/s
P_{wf}	bottom hole flowing pressure, Pa
S	skin factor
k	coefficient of permeability, m^2
ρ	acceleration of gravity, m/s^2
W	mass flow rate, kg/s
$p(r,t)$	pressure at distance r and time t, Pa
m	slope of semilog straight line, Pa/cycle
μ_t	mixture (steam+water) dynamic viscosity, Pa.s
μ_w	water dynamic viscosity
μ_s	steam dynamic viscosity
k_{rs}	relative permeability of water
k_{rs}	relative permeability of steam
ν_t	mixture kinematic viscosity, m^2/s
ν_w	water kinematic viscosity
ν_s	steam kinematic viscosity
ρ_s	steam density, kg/m^3
ρ_w	water density
ρ_t	mixture density
T	transmissivity, $m^3/Pa.s$
S	storage coefficient
H	enthalpy, kJ/kg

1 INTRODUCTION

1.1 Scope of the work

This report is a part of the author's work during his training in reservoir engineering at the United Nations University Geothermal Training Programme at Orkustofnun, the National Energy Authority of Iceland, during the period April to October 1985.

The six month training period commenced by a six week introductory lecture course including subjects such as surface and borehole geology, surface and borehole geophysics, geochemistry, drilling technology, hydrology, reservoir engineering and geothermal utilization. The following six weeks were devoted to specialized training in reservoir engineering and borehole geophysics with lectures and practical field exercises.

The author was also given an opportunity to participate in a field excursion to the main low and high temperature geothermal fields in Iceland and thus to experience various utilizations of geothermal energy around the country.

The remaining part of the training period was devoted to the preparation of this report including one week participation in practical field work in the Krafla-Hvitholar area to study geothermal well pressure recovery, but this area is the target area for this reserach project.

It is the author's belief that good use will be made of this training upon return to his home country.

1.2 The Krafla-Hvitholar geothermal area

The Krafla geothermal field is located in the Neovolcanic zone in northeastern Iceland. The Neovolcanic zone is characterized by fissure swarms and central volcanoes (Saemundsson, 1974, 1978). The Krafla central volcano developed a caldera during the last interglacial period, Since then the caldera has been filled with hyaloclastites

and lavas. The caldera measures about 8x10 km. Beneath the caldera lies a magma chamber, at a depth of 3 to 7 km. To date 23 wells have been drilled in the Krafla geothermal field. They are located in three main production areas, the Leirbotnar area, the southern slopes of Mt. Krafla and the Hvitholar area. Their location is shown in Fig. 1.

Hvitholar (White hills) draw their name from the white colour of altered clay on the surface. The Hvitholar area is rather small (between 0.2 and 0.3 km^2) and situated near the south rim of the Krafla caldera, 1.5 km away from the Krafla power plant. Geological studies at the surface indicate two active fracture trends in the area. One the N-S trend of the main fissure swarm and the other a E-W fracture trend connected with the southern edge of the caldera. The location of the wells and a general map of the area is shown in Figure 2.

For the last decades no active surface manifestations were observed at Hvitholar, but in 1979 the area became active again with steaming of the ground. Surface menifestations in Hvitholar are associated with ground alterations. Rock samples from drillholes show that hyaloclastite is the governing rock type in the uppermost 1000 m, but basalt lavas below that.

Geophysical measurements were carried out in the Hvitholar area during the period June to August 1983. Schlumberger soundings and head-on resistivity profiling as well as magnetic measurements were performed over an area of 1.6 km^2. By using Schlumberger soundings and head-on profiling along the same lines, better information of the resistivity and the geological sequences down to a depth of 400 to 800 meters was gained.

Resistivity measurements indicate a rather small low resistivity area coinciding with the hot ground. The resistivity measurements also indicate that the geothermal area is confined to a limited upflow channel (Bjornsson, 1984).

Geochemical analysis of hot water samples from the Hvitholar area have no magmatic overprint. Gas geothermometry indicates a reservoir temperature > 240°C. The gas concentration is very low unlike that of the other production wells in Leirbotnar and the southern slopes.

1.3 Summary of the drilling history

Three wells were drilled in the Krafla-Hvitholar area in 1982 and 1983. The wells are KJ-21, KJ-22 and KJ-23, with a depth of 1200 m, 1878 m and 1968 m respectively.

Well KJ-22 was directionally drilled to the west. The aim of the directional drilling was to intersect several N-S trending fissures and to investigate the western edge of the geothermal field (Fig. 2). Information on casings, dates of drilling, location of main aquifers, total drill depth, inclination of wells and total drilling time is given in Table 1.

TABLE 1: Well completion and aquifer location

Year of drilling	Time of drilling (days)	Casing 13 3/8"	9 5/8"	7"liner	Well
1982	38	to 286	-	118	KJ-21
1983	61	to 154	to 567	185	KJ-22
1983	40	to 196	to 536	-	KJ-23

Main aquifer location (m)	Drilled depth (m)	Inclination (degrees)	Well
570 700 925 970	1200	Fairly vertical	KJ-21
600 960 1050 1080 1165 1270 1300 1335 1600 1750 1800 1845	1878	37.90	KJ-22
600 700 1290 1660	1968	Fairly vertical	KJ-23

N.B. The 7" liner pulled out in 1984 and 9 5/8" blind and slotted casing sunk in well KJ-21. Total time spent for drilling was 24 day, the rest for repair (KJ-21).

2 WELL TESTING

2.1 The basic pressure diffusion equation

The differential equation for fluid flow in porous media, the pressure diffusion equation, is a combination of the law of conservation of mass, an equation of state and Darcy's law. Assuming horizontal flow, negligible gravity effects, a homogenous and isotropic porous medium, a single fluid of small and constant compressbility and a small pressure gradient the diffusion equation can be written in radial coordinates

$$\frac{\partial^2 P}{\partial^2 r} + \frac{1}{r}\cdot\frac{\partial P}{\partial r} = \frac{\phi\mu C_t}{k}\cdot\frac{\partial P}{\partial t} \qquad (1)$$

The parameters μ, C_t, k and ϕ are considered independent of pressure.

The radial diffusion equation can be written in terms of dimensionless variables which are defined as follows:

$$P_D(t_D,r_D) = \frac{2\pi kh}{q\mu}\,(P_i - P(r,t)) \qquad (2)$$

$$t_D = \frac{kt}{\phi\mu C_t r_w^2} \qquad (3)$$

$$r_D = \frac{r}{r_w} \qquad (4)$$

Combining equations (1) through (4) gives:

$$\frac{\partial^2 P_D}{\partial^2 r_D} + \frac{1}{r_D}\cdot\frac{\partial P_D}{\partial r_D} = \frac{\partial P_D}{\partial t_D} \qquad (5)$$

This is the dimensionless radial pressure diffusion equation. The derivation and solutions of the radial diffusion equation with various initial and boundary conditions is available in the literature (Earlougher, 1977, Grant, et.al, 1982 and Matthews and Russel, 1967).

2.2 Methods of well test analysis

The radial diffusion equation is the fundamental equation for well test analysis. Different methods of analysis are based on solutions of this equation with various inital and boundary conditions. The following methods will be applied in this report:

2.2.1 The semilogarithm method

For the infinite reservoir with boundary and initial conditions as follows:

(1) $P_D = 0$ at $t_D = 0$, for all r_D

(2) $P_D = 0$ at $r_D = \infty$, for all t_D

(3) $\lim_{r_D \to o} r_D \frac{\partial P_D}{\partial r_D} = 1$ $t_D > 0$

the solution of Eq. 5 is then the exponential integral solution given by

$$P_D(t_D, r_D) = -\frac{1}{2} Ei\left(-\frac{r_D^2}{4t_D}\right) \qquad (6)$$

Eq. 6 can be approximated when $t_D/r^2{}_D \geq 25$.

$$P_D(t_D, r_D) = \frac{1}{2}\left[\ln\frac{t_D}{r_D^2} + 0.80907\right] \qquad (7)$$

This is called the logarithmic approximation. Substituting Eq. 7 into Eq. 2 gives

$$P(r,t) - P_i = -\frac{q\mu}{4\pi kh}\left[\ln\frac{t_D}{r_D^2} + 0.80907\right] \qquad (8)$$

An additional pressure drop due to the so called skin effect around the well can be added to the solution given by Eq. 8

$$\Delta P_{skin} = \frac{q\mu}{2\pi kh} \cdot S \qquad (9a)$$

where S is the skin factor for the well. The change in flowing bottom hole pressure, $P_i - P_{wf}$, is then given by $(r=r_w)$

$$P_i - P_{wf} = \frac{q\mu}{4\pi kh}\left[\ln t + \ln\left(\frac{k}{\phi\mu C_t r_w^2}\right) + 0.80907 + 2S\right] \qquad (9b)$$

When the pressure change given by Eq. 9b is plotted against time on the semilogarithmic scale, a straight line will be obtained having a slope equal to

$$m = \frac{2.303q\mu}{4\pi kh} \qquad (10)$$

This can be written in terms of mass flow rate W:

$$m = \frac{2.303W\mu}{4\pi kh\rho} \qquad (11)$$

where $W = q \cdot \rho$

Once the slope is identified, the transmissivity can be estimated as follows:

$$T = \frac{kh}{\mu} \quad \text{or} \quad T = \frac{2.303W}{4\pi m\rho} \qquad (12)$$

Extending the straight line to $\Delta P = 0$ and defining the corresponding time by t_o, Eq. 8 gives an expression for formation storage:

$$\phi C_t h = \frac{2.246kt_o}{\mu r_w^2} h \qquad (13)$$

The storage coefficient is defined as

$$S = \phi C_t h \rho g = \frac{2.246kht_o}{\mu r_w^2} \rho g \qquad (14)$$

Equations 12 and 13 are the working equations in the semilog analysis technique for estimating the transmissivity and the formation storage. After transmissivity and storage have been estmated it is possible using Eq. 9b to estimate the skin effect at the well by:

$$S = 1.1513 \left[\frac{P_i - P_t}{m} - \log \frac{k}{\phi \mu C_t r_w^2} - \log t - 0.351\right]$$

where $P_i - P_t$ is the pressure drop after t seconds.

If we put t = 60 seconds

$$S = 1.1513 \left[\frac{P_i - P_{1min}}{m} - \log \frac{k}{\phi \mu C_t r_w^2} - 2.13\right] \qquad (15)$$

where P_{1min} is the pressure at t = 60 seconds.

2.2.2 The type curve matching method

A straight line in the semilogarithmic plot can sometimes be difficult to identify. Due to effects such as the skin effect, wellbore storage effects and other effects, the type curve matching has prooven to be useful for estimating the transmissivity, storage and skin effect.

Taking the logarithm of both sides of equations 2 and 3 results in

$$\log \frac{q\mu}{2\pi kh} + \log P_D = \log \Delta P$$

$$\log \frac{q\mu}{2\pi kh} = \log \frac{\Delta P}{P_D} \quad \rightarrow \quad \frac{q\mu}{2\pi kh} = \frac{\Delta P}{P_D}$$

$$\frac{kh}{\mu} = \left(\frac{q}{2\pi} \frac{P_D}{\Delta P}\right)_{M.P} \qquad (16)$$

$$\log t_D = \log \frac{k}{\phi \mu C_t r_w^2} + \log t$$

$$\log \left(\frac{t}{t_D}\right) = \log \left(\frac{\phi \mu C_t r_w^2}{k}\right) \qquad (17)$$

$$C_{t\phi} = \frac{k}{\mu r_w^2} \cdot \left(\frac{t}{t_D}\right)_{M.P.}$$

$$C_t \cdot \phi \cdot h = \frac{kh}{\mu r_w^2} \cdot \left(\frac{t}{t_D}\right)_{M.P.} \qquad (17)$$

where M.P. indicates a match point.

The type curve is now taken and the observed data is plotted on the same scale on a tracing paper. The tracing paper is then shifted until a best fit is obtained with one of the curves; the axes kept parallel while shifting in order to match the points. After the points match one of the curves, taking any convenient point called a match point on the ΔP versus Δt log, the log plot determines the corresponding P_D and t_D, then using Eq. 16 and Eq. 17 the reservoir parameters can be determined.

2.2.3 Jacobs's and Rorabaugh's method

Jacob's (1950) and Rorabaugh's (1953) method was developed in ground-water hydrology to determine the transmissivity and turbulent pressure drop in the vicinity of the well. This method can also be used in geothermal reservoirs to determine transmissivity by pumping water at different flow rates and observing the corresponding water level

The equation which relates the drawdown and volumetric flow rate was given by Jacob and Rorabaugh as

$$S_w = BQ + CQ^2 \qquad (18)$$

where B = coefficient of laminar pressure drop m/(l/s); C = coefficient of turbulent pressure drop m/(l/s)^2; Q = volumetric flow rate (l/s); S_w = drawdown in flowing well or water level in the injection well (m).

S_W/Q plotted against Q on a linear scale will give a straight line from which B and C in Eq. 18 can be determined. The value of B can be used to determine the transmissivity of the formation when the skin effect (S) is equal to zero.

In the case of infinite reservoirs the equation relating the drawdown and the volumetric flow rate can be written as:

$$S_W = \frac{Q \cdot 10^{-3}}{4\pi T \rho g} \cdot W(u) + CQ^2 \qquad (19)$$

where W(u) is the well function, T the transmissivity and

$$u = \frac{r_w^2 \cdot S}{4Tt\rho g} \qquad (20)$$

For $u < 0.01$

$$S_W = \frac{Q \cdot 10^{-3}}{4\pi T \rho g}(-\ln u - 0.5772) + CQ^2 \qquad (21)$$

Solving for B

$$B = \left(\frac{-\ln u - 0.5772}{4\pi T \rho g}\right) \cdot 10^{-3} \qquad (22)$$

Substituting Eq. 20 in Eq. 22 gives

$$T = \frac{\left[-\ln\left(\frac{r_w^2 \cdot S}{4Tt}\right) - 0.5772\right]}{4\pi B \rho g} \cdot 10^{-3} \qquad (23)$$

This equation is the working equation used to determine the transmissivity of the formation by Jacob's and Rorabaugh's method.

The methods described in sections 2.2.1, 2.2.2 and 2.2.3 are used in the analysis of well test data from wells KJ-21, KJ-22 and KJ-23.

3 INJECTION TESTS

3.1 The purpose of injection tests in geothermal wells

An injection test in a newly drilled well gives the first indications of the geothermal reservoir properties and future productivity of the well. The test is used to estimate the transmissivity (the ability to conduct fluid) and storability of the aquifers as well as the skin effect around the well.

3.2 Implementation of the injection test

In this section the procedure and the setup used during injection tests in the Krafla-Hvitholar geothermal area will be discussed. The injection test is usually carried out during the well completion phase after the liner has been lowered into the well. The setup used for the injection test at Krafla-Hvitholar is shown in Fig. 3. Prior to the test a steady pumping rate (20-25 l/s) is maintained for several days to obtain stable pressure conditions in the well.

Before conducting an injection test the following steps must be taken: 1) Design the test indicating which parameters are to be measured, e.g. pressure or water level. Determine the measurement depth; 2) Check the calibration and working conditions of the instruments used; 3) Check the stable condition of the well; 4) Place the measuring device in the well; 5) Start the test.

At the beginning of the test in the Hvitholar wells, a pressure transducer (sensor) is lowered to a depth of 200 m. Continuous measurements are received at the surface. After some base values of the pressure have been taken, the injection test is started by observing the pressure fall-off when the injection is discontinued for about 2-3 hours (112 min, 156 min and 195 min in wells KJ-21, KJ-22 and KJ-23 respectively). The injection rate is then increased in steps of 1-3 hour duration, and the change in pressure recorded. The test is then completed by retrieving

the pressure transducer to the surface and closing the well.

3.3 Injection tests of the Hvitholar wells

3.3.1 Well KJ-21

The injection test started on 14th September 1982 with a pressure sensor being lowered to 200 m depth. The inital pressure was 10.87 bar. This pressure had been maintained prior to the first fall-off test by pumping 19.64 l/s of cold water. The pressure fall-off test lasted for 112 minutes followed by a step injection. The flow rate used was 36.14 l/s and 58.57 l/s.

The results of the injection test which was carried out in well KJ-21 have the following non-theroretical features:

1) Pressure recovery during the fall-off; 2) Unit slope in the early time data (log-log plot); 3) Fluctuations in the late time data.

These features can be explained as: 1) fluid flow between aquifers; 2) wellbore storage effect and some sort of interference. When fluid flow takes place between aquifers at different temperature the pressure transient changes due to the density variations. The density variation accounted for the fast thermal recovery in that section of the well.

During pumping of cold water into a well, the effect of pumping is not directly transmitted into the formation due to the effects of the free liquid level in the well, the wellbore storage effect (Earlougher, 1977). This causes a time lag in the pressure response. Wellbore storage effects can be checked by plotting pressure changes against the time on a log-log scale. In the wellbore storage effect dominated part of the data, such a plot has a unit slope. Therefore the wellbore storage effect can be recognized by the unit slope of the early transient pressure data.

To eliminate the wellbore storage effect part of the data, the change in pressure for well KJ-21 was plotted against the change in time on a log-log scale. The data collected during the pressure fall-off and the step injection were then analysed by using the semilog method, type curve matching, and Jacob's and Rorabough's method.

As shown in Figure 4, where the pressure at 200 m depth is plotted against change in time on a semilog scale, (taking each step seperately), the slope is found to be 0.41 bar/cycle (36.141 l/s). The corresponding transmissivity (of the well) is $kh/\mu = 16.2 \times 10^{-8}$ $m3/P_a \cdot s$.

Fig. 6 shows the change in water level against the flow rate. The slope is obtained from the straigth line drawn through the points (B = 1.1 m/(l/s)). Assuming $S=10^{-4}$ the transmissivity can be determined, based on Eq. 23, by iterations:

$$\frac{kh}{\mu} = 13.1 \times 10^{-8} m3/P_a \cdot s.$$

A log-log plot of the pressure for the 36 l/s step is also shown is Figure 5. This data was analysed by type-curve matching. A satisfactory match was obtained using a type curve with wellbore storage effect and skin included by Agarwal et al. (1970). Transmissivity was found to be $kh/\mu = 13.2 \times 10^{-8}$ $m3/P_a \cdot s$.

3.3.2 Well KJ-22

An injection test was carried out in well KJ-22 on 14th July 1983. A pressure sensor was lowered to a depth of 200 m. Prior to the test a steady pumping rate of 26.87 l/s was used to maintain a stable pressure in the well. The injection test started by a pressure fall-off followed by step injection. The flow rates were 12.23 l/s, 24.46 l/s, 36.88 l/s and 48.0 l/s.

The injection test data were again analysed by using the semilog method, type curve matching and Jacob's and Rorabough's method. The slope and the calculation of transmissivity and formation storage are shown in Figs. 7, 8 and 9.

The pressure at the end of each step was plotted against the flowrate. The resulting curve is shown in Fig. 10. The break in the two straight lines appears to happen at the flow rate that stopped the interzonal flow between aquifers. Therefore the deviation of the curve from the straight line is not because of fracturing, but is due to interzonal flow.

3.3.3 Well KJ-23

An injection test was performed in well KJ-23 during the 21st and 22nd of September, 1983 with the pressure sensor lowered to a depth of 200 m. The test commenced by the first pressure fall-off, the flow rate before the fall-off being 6.12 l/s. This was followed by the pumping of cold water (20°C) at 13 l/s. Unfortunately after some time had elapsed the water level reached the surface (backfilling). Because of the backfilling, pumping was stopped and the second fall-off test conducted which lasted 200 minutes. After the second fall-off test ended, variable flow rates were used while the changes in pressure were monitored at the well head.

As shown in Figs. 11, 12 and 13, the transmissivity and formation storage are found using the methods mentioned above. The backfilling characteristics of well KJ-23 are associated with poor permeability around the well.

3.4 Summary of the injection test analysis

The injection test data were interpreted using well known techniques discussed in chapter 2.2. Table 2 gives a summary of the calculated values of the transmissivity (kh/μ) and the formation storage ($C_{t\phi h}$) for different flow rates and test analaysis methods. Results indicate

transmissivity values for wells KJ-21, KJ-22 and KJ-23 in decreasing sequence. This is in a good agreement with the production of the wells. Well KJ-21 is the best producing well at Hvitholar, whereas well KJ-23 is not producing at all at the present time.

The data from discharge measurmements, in wells KJ-21 and KJ-22 were analysed using James (1962) lip pressure method, which is the the most widely used method. The method relates the discharge enthalpy, discharge pipe area, flow rate and lip pressure (see Grant, et al., 1981). Results show high mass flow rate, steam mass fraction and enthalpy for well KJ-21. The output characteristics of the productive wells at Hvitholar are shown in Fig. 15.

TABLE 2: Transmissivity and formation storage values for wells at Hvitholar

Transmissivity 10^{-8} m3/Pas

Well No.	Semilog	Type curve	Jacob's and Rorabaugh's	Flow rate
KJ-21	16.2	13.2	13.1	36.14
KJ-22	3.13			48
	5.7	3.3	5.9	36.88
	2.04			24.46
KJ-23	7.74	0.77	1.3	13.0
	0.8			6.12

Formation storage 10^{-8} m/Pa

Well No.	Semilog	Type curve	Flow rate
KJ-21	1.31	1.08	36.14
KJ-22	2.4	5.6	24.46
KJ-23	5.1	9.2	13.0

4 PRESSURE RECOVERY TESTS

4.1 Introduction

To date three wells have been drilled in the Hvitholar geothermal area of which two are productive. During the summer of 1985 the wells at Hvitholar were closed for a period of three months. During this time pressure and temperature measurements were conducted in all three wells. The aim of the test was to obtain data for an evaluation of the reservoir.

The test was performed during the period from the middle of May to the middle of August, 1985. Prior to the test, well KJ-21 had been producing while the other two were closed. Pressure and temperature logs were run in all the wells (KJ-21 was closed during the measurement). After this KJ-21 was set to discharge for about five days whereafter pressure measurements were conducted at a depth of 800 m in well KJ-22 and KJ-23 (this depth was selected because of the water level and proximity to the main aquifers). On May 15th well KJ-21 was closed and the pressure recovery measurements were carried out. On August 15th well KJ-21 was again placed on discharge and pressure monitored in wells KJ-22 and KJ-23.

4.2 Analysis of pressure recovery data

The pressure recovery was observed in the Hvitholar wells at a depth of 800 m. Prior to the test all the wells had been logged for temperature and pressure in order to obtain a base value. During this test the interference between wells was also checked, by discharing well KJ-21 and monitoring the pressure in the other two wells. The results indicate an interference between wells KJ-21 and KJ-23 (a drop of 1 bar) and no interference in the case of KJ-22.

4.2.1 Well KJ-21

The pressure build-up data from this well is shown in Fig. 14. The discharge enthalpy (1643 kJ/kg) of well KJ-21 is greater than the enthalpy of water at the maximum temperature (268°C) measured in the well. This is an indication of two phase inflow. In pressure transient analysis for two phase inflow, the mixture (steam + water) density, the mixture viscosity and relative permeability should be used for the evaluation of reservoir parameters.

Dynamic viscosity of the mixture is defined by (Grant et. al, 1982).

$$\frac{1}{\mu_t} = \frac{k_{rw}}{\mu_w} + \frac{k_{rs}}{\mu_s} \qquad (25)$$

the kinematic viscosity by

$$\frac{1}{\nu_t} = \frac{k_{rw}}{\nu_w} + \frac{k_{rs}}{\nu_s} \qquad (26)$$

and the mixture density by (Grant, et al, 1982)

$$\frac{1}{\rho_t} = \frac{1}{H_{sw}} \left[\frac{H_t - H_w}{\rho_w} + \frac{H_s - H_t}{\rho_s}\right] \qquad (27)$$

$$\frac{1}{\rho_t} = \frac{x}{\rho_w} + \frac{1-x}{\rho_s} \qquad (28)$$

$$x = \frac{H_t - H_w}{H_{sw}} \qquad (29)$$

where: x = steam fraction; H_t = total discharge enthalpy, kJ/kg; H_s = steam enthalpy; H_w = water enthalpy; H_{sw} = $H_s - H_w$ latent heat. For other notations see list of symbols.

The enthalpy of the steam-water mixture is given by

$$H_t = \left(\frac{H_w k_{rw}}{\nu_w} + \frac{H_s k_{rs}}{\nu_s}\right) \cdot \nu_t \qquad (30)$$

subsituting Eq. 26 in Eq. 30 and rearranging

$$\frac{k_{rw}}{k_{rs}} = \frac{\nu_w}{\nu_s}\left(\frac{H_s - H_t}{H_t - H_w}\right) = \frac{\nu_w}{\nu_s}\cdot\frac{1-x}{x} \qquad (31)$$

The mixture density can be determined as follows, applying Eqs. 28 and 29. The flowing enthalpy H_t = 1643 kJ/kg.

At the temperature 260°C (from steam table), H_s = 2796.4 kJ/kg; H_w = 1134.9 kJ/kg; H_{sw} = 1661.5 kJ/kg; ρ_s = 23.7 kg/m3; ρ_w = 783.9 kg/m^3; μ_w = 104.8×10^{-6} $P_a\cdot s$; μ_s = 17.9×10^{-6} $P_a\cdot s$; ν_w = 0.134×10^{-6} m^2/s; ν_s = 0.755×10^{-6} m^2/s.

Thus

$$x = \frac{1643-1134.9}{1661.5} = 0.31$$

From Eq. 28

$$\frac{1}{\rho_t} = \frac{x}{\rho_s} + \frac{1-x}{\rho_w} = \frac{0.31}{23.7} + \frac{0.69}{783.9} \qquad \text{and} \quad \rho_t = 71.6 \text{ kg/m}^3$$

Using Eq. 31

$$\frac{k_{rw}}{k_{rs}} = \frac{0.134\times10^{-6}}{0.755\times10^{-6}}\cdot\left(\frac{1 - 0.31}{0.31}\right) = 0.40$$

Assuming Grant relative permeability relation, that is $k_{rw} + k_{rs} = 1$, then $k_{rs} = 0.71$ and $k_{rw} = 0.29$.

Using these relative permeability values in Eq. 25 the dynamic and kinematic viscosity of the mixture can be obtained

$$\frac{1}{\mu_t} = \frac{K_{rw}}{\mu_w} + \frac{K_{rs}}{\mu_s} = \frac{0.29}{104.8\times10^{-6}} + \frac{0.71}{17.9\times10^{-6}}$$

$\mu_t = 2.4\times10^{-5}$ $P_a\cdot s$ and $\nu_t = 3.3\times10^{-7}$ m^2/s.

Based on the slope of the straight line portion of Fig. 14 and the mixture parameters calculated above, the transmissivity can be estimated.

$$\frac{k_h}{\mu_t} = \frac{2.303W}{4\pi m \rho_t} = \frac{2.303 \times 33.5 \text{ kg/s}}{4\pi \times 4.45 \times 10^5 P_a \times 71.6 \text{ kg/m}^3} = 19.3 \times 10^{-8} \text{ m}3/P_a \cdot s$$

$k_h = 19.3 \times 10^{-8} \times 2.4 \times 10^{-5} = 4.6 \times 10^{-12}$ m3 and the formation storage ($t_o = 3.24 \times 10^3$ S).

$$C_{t\phi h} = \frac{2.246 T t_o}{\nu_w^2} = \frac{2.246 \times 19.3 \times 10^{-8} \times 3.24 \times 103}{(0.108)^2} = 0.12 \text{ m/Pa}$$

4.3 Summary and results

The transmissivity value ($19.3 \times 10^{-8} m3/P_a \cdot s$) obtained based on the pressure recovery test for well KJ-21 is of the same order of magnitude as that obtained from the injection test (16.2×10^{-8} m3/$P_a \cdot s$), but the formation storage is much higher. This reflects the fact that the two phase fluid is much more compressible than the liquid phase.

In the case of the other two wells (KJ-22 and KJ-23) the data collected during the summer 1985 is not suitable for analysis based on the use of the standard methods considered here.

5 TEMPERATURE AND PRESSURE LOGS

5.1 Introduction

A log is defined as a continuous measurment carried out in a borehole. Temperature and pressure logs give important imformation about the condition of the well and the reservoir. The temperature log from a borehole reflects the temperature of the reservoir, location of aquifers, temperature gradients and heat flow. The pressure logs will reflect the reservoir pressure response of the field to production and location of strong aquifers. It is possible to determine the phase of the fluid in the well based on measured temperature and pressure.

In the following sections temperature and pressure logs taken from three wells in the Krafla-Hvitholar geothermal area will be discussed.

5.2 Temperature and pressure logs from the Hvitholar wells

5.2.1 Well KJ-21

Several temperature and pressure logs exist from well KJ-21. The temperature logs were measured during three periods; the drilling period, the recovery period after drilling and finally just after the start of production. The most important of these logs are shown in Figs. 16, 17 and 18. On the first figure (Fig. 16), two logs are shown. The first one is measured at the completion of the well when 48 l/s of water were pumped into the well and the second log is measured 2.5 hours after pumping was stopped.

The thermal recovery of the well was fast due to fluid inflow in the upper part of the well, and the location of the aquifers can be easily pointed out from the log. All aquifers above 600m add fluid into the well. The flow continues downhole and into the aquifers below 600 m depth. Note that the negative temperature gradient in the interval 600-950 m indicates the flow direction as the inflow temperature at 600 m increases in time, whereas the

sudden drop in temperature at about 1000 m depth indicates the lower end of the cross flow region. Below this depth the well seems to be more or less non-permeable (only small aquifers).

Fig. 17 shows several temperature logs from the heating-up period of well KJ-21. All the logs show a similar pattern as the one discussed above. The main difference is the shift of the profiles towards higher temperatures as the well heats up. It is also worth noting that the cross flow in the later measurements extends almost to the bottom of the well indicating that an aquifer is located there. Due to the cross flow in the well, it is only possible to use the temperature logs during recovery to estimate reservoir temperatures down to 600 m, where the main crossflow starts, and at the bottom of the well, below the crossflow region. The logs indicate that the reservoir temperature at 600 m depth is higher than 250°C and that of the bottom hole temperature exceeds the measured temperature. The extrapolated bottom hole temperature, using Horne's method, is 221°C.

In order to get a better determination of the reservoir temperatures around well KJ-21, some temperature logs were run after the well had discharged. On each occasion the well was kept closed while the measurement was done. Unfortunately the well plugged at 641 m depth, so only one bottom hole temperature reading was obtained. This was after five days discharge, giving a bottom hole temperature of 200°C (see Fig. 18).

During thermal recovery of well KJ-21, the pressure in the well was monitored by running several pressure logs (Fig. 19). The pivot point was found in the crossflow interval at 700 m depth, indicating that of the main feed zones at 570, 795 and 925 m depth the one at 570 m depth is the most permeable aquifer of the well. The thermal recovery of the well (Fig. 17), was very fast above the pivot point when pumping stopped at the end of drilling. It is thus not surprising to see effects of thermal recovery and crossflow (see section 3.3) in the injection data.

In order to summarize the temperature and pressure data from well KJ-21, Fig. 20 is drawn. It shows the boiling point curves (temperature and pressure) and the reeservoir values of the temperatures and pressure determined from the logs. Boiling conditions exist in the reservoir down to at least 600 m depth, whereas at the bottom (1200 m) temperature is far below the boiling point curve (Fig. 20). Although the reservoir temperature profile of well KJ-21 is poorly defined, Fig. 20 shows an educated guess of how this profile could be.

5.2.2 Well KJ-22

There are several temperature and pressure logs available which were measured during drilling, during thermal recovery and finally right after the beginning of production. The temperature logs are shown on Figs. 21 and 22. Fig. 21 shows the temperature profiles conducted during thermal recovery. This figure clearly illustrates the potential feed points (indicated by arrows).

Thermal recovery in the upper part of well KJ-22 is fast, which is associated with circulation of fluid between existing aquifers in the well. Note that the temperature decreases with depth in the interval 600-1200 m and then temperature is constant below 1200 m depth. The inflow at 600 m depth moves down hole, and mixes with much colder inflow at 1250 m, accounting for the sudden temperature drop in the profile (the main inflow is probably at 1250 m depth).

The second temperature profile (83/07/19), (Fig. 21), is similar to the first one, except that the latter one shifts to a higher temperature. The third profile (Fig. 21) indicates that crossflow is no longer of importance as the fluid becomes lighter and can not move downhole any more. Gas and steam rise up and accumulate above a higher density fluid. The temperature logs illustrate that the reservoir temperature above 700 m exceeds 250°C.

In order to get a better determination of the reservoir temperatures around well KJ-22, temperature logs were measured after discharge (Fig. 22). The temperature of the well in the uppermost 700 m decreases after discharge. This is due to boiling in the well during discharge and also due to flow of colder fluid from the deeper aquifers of the well.

During thermal recovery of well KJ-22, the pressure of the well was monitored by running several pressure logs (Fig. 23). The pivot point (1100 m depth) of the well lies near the main inflow region, indicating that the aquifer at a depth of 1250 m is the most productive aquifer of the well.

The temperature and pressure data for well KJ-22 are summarized in Fig. 24. The plot shows the boiling point curves (temperature and pressure) and reservoir values, furthermore the figure illustrates that the temperature of the reservoir below 600 m is far below boiling conditions.

It was impossible to determine the exact reservoir temperature, due to the existing flow between different aquifers. However, the reservoir temperarture profile could possibly be as shown in Fig. 24.

5.2.3 Well KJ-23

Well KJ-23 is the deepest well drilled in the Krafla-Hvitholar geothermal area. Numerous logs are available for this well, dating back to the time of drilling (1983),and from the thermal recovery period, which is now in effect as this is a non-producing well. Temperature measurements from 1983 and 1984 are shown in Fig. 25. Feeder zones are easily identified in the logs and indicated by arrows. The well has similarities to the other two wells, in that the maximum tempearture recorded is found at a depth around 600 m.

The reservoir temperature of the well at 600 m is greater than 255°C and 245°C at the bottom. Pressure logs conducted in this well indicate the pivot point, prevailing at a

depth of 600 m (Fig. 26). The tempearture and the pressure profiles are summarized in Fig. 27. The reservoir temperature is also clearly defined.

5.3 Temperature and pressure distribution in the Hvitholar geothermal area

A temperature cross-section for the Hvitholar field in an E-W direction is shown in Fig. 28. The figure indicates an S-shaped temperature trend in the Hvitholar geothermal area. The temperature increases towards the east and well KJ-21 appears to be near the up-flow zone. The reservoir pressure profiles on Fig. 28 show a higher pressure in well KJ-21 compared to wells KJ-22 and KJ-23. This reflects a heat flow direction towards the west.

6 SUMMARY AND CONCLUSIONS

1. The Krafla-Hvitholar area is the smallest (0.2-0.3 km^2) of the three production areas of the Krafla geothermal system. It is located near the south margin of the Krafla caldera. Three wells have been drilled in the area, wells KJ-21, KJ-22 and KJ-23.

2. The Krafla-Hvitholar reservoir appears to be liquid-dominated with steam caps around the wells. This is characterized by a subhydrostatic pressure gradient in the upper most 600 m

3. Temperature profiles in the area are characterized by a temperature reversal with the maximum temperature of about 260°C at a depth of 600 m. The direction of heat flow is towards the west with well KJ-21 located near the upflow zone.

4. Pressure transient tests, injection tests as well as a pressure build-up test in well KJ-21 indicate the highest transmissivity of $1.3\text{-}1.9 \times 10^{-7} m^3/P_a \cdot s$ near well KJ-21 and the lowest transmissivity of 0.8 $m^3/P_a \cdot s$ near well KJ-23. This is clearly reflected in the productivity of the wells.

ACKNOWLEDGEMENTS

The author would like to express his gratitute to Dr. Ingvar Birgir Fridleifsson for his successful organization and completion of the 1985 session of the UNU Geothermal Training Programme.

The author is very much indepted to Mr. Benedikt Steingrimsson for his continous supervision and discussion; to Dr. Gudni Axelsson for carefully reading the manuscript and giving valuable suggestions; to Mr. Gudjon Gudmundsson for collecting all of the data and giving practical instructions.

My special thanks go to Mr. Sigurjon Asbjornsson for his practical assistance during our stay and for typing and editing the report; to Halldora Hreggvidsdottir for translating some of the Icelandic papers into English for me and lastly to Ms. Erla Kristjansdottir for drafting most of the figures for this report.

The help of the teaching staff of the UNU Geothermal Training Programeme is acknowledged. Finally thanks to the Fellows of the UNU 1985 for the good comraedship during this period.

REFERENCES

Agarwal, R., Al-Hussainy, R., Ramey, H.J., Jr., (1970): An investigation of wellbore storage and skin effects in unsteady liquid flow, 1. An analytical treatment, SPE Journal, pp 279.

Armannsson, H., Steingrimsson, B, (1984): Krafla, well KJ-22 heating up period, initial discharge test and discharge. NEA Report OS-84008/JHD-02B, (in Icelandic).

Armannsson, H., Benjaminsson, J., Steingrimsson, B., (1983): Krafla, well KJ-21 heating-up period initial discharge test and discharge, NEA Report OS-83013/JHD-03B, (in Icelandic), 26 pp.

Bjornsson, A., Eyjolfsson, B., Gunnarsson, K., Saemundsson, K., Arnason, K., (1984): A Geological and geophysical reconnaissance at the Hvitholar area, Krafla, (in Icelandic).

Bodvarsson, G.S., Benson, S.M., Sigurdsson, O., Halldorsson, G.K., Stefansson, V., (1981): Analysis of well test data from the Krafla geothermal field, Iceland. Proc. 7th Workshop Geothermal Reservoir Engineering, Stanford Univ., Calif., 71-76.

Bodvarsson, G.S., Benson, S.M., Sigurdsson, O., Stefansson, V., Eliasson, E.T., (1984): The Krafla geothermal field, Iceland, 1. Analysis of well test data, Water Resources Research, V. 20, No. 11, 1515-1530.

Earlougher, R.C., (1977): Advances in well test analysis, SPE monograph, V. 5, Dallas, 245 pp.

Grant, M.A., (1979): Interpretation of downhole measurements in geothermal wells, Rep. No. 88.

Grant, M.A., Donaldson, I.G. and Bixley, P.F., (1982): Geothermal reservoir engineering, Academic Press, N.Y., 369 pp.

Gudmundsson, A., Steingrimsson, B., Fridleifsson, G.O., Tryggvason, H., Sigurdsson, O., (1982): Krafla, well KJ-21, Drilling of production part of the well from 217 to 1200 m, NEA Report OS-82119/JHD-35B, 26 pp, (in Icelandic).

Gudmundsson, A., Steingrimsson, B., Sigurdsson, D., Gudmundsson, G., Fridleifsson, G.O., Tryggvason, H., Sigurdsson O., (1983): Krafla, well KJ-22, Drilling of production part of the well, NEA Report OS-83071/JHD-22B, 21 pp, (in Icelandic).

Gudmundsson, A., Steingrimsson, B., Gudmundsson, G., Fridleifsson, G.O., Sigvaldason, H., Tryggvason, H., Sigurdsson, O., (1983): Krafla, well KJ-23. Drilling of production part of the well. NEA Report OS-83082/JHD-27B, 23 pp, (in Icelandic).

Jacob, C.E. (1950): Flow of groundwater in engineering hydraulics (H. Rouse, ed.), Wiley, N.Y., Chap. 5, 321-386.

James, R., (1962): Steam water critical flow through pipes, Inst. of Mech. Engr's Proc., V. 176, No. 26, 741.

Kjaran, S.P. and Eliassson, J., (1983): Geothermal Reservoir Engineering Lecture Notes, UNU Geothermal Training Programme, Report No. 1983-2, 250 pp.

Matthews, C.S. and Russel, D.G., (1967): Pressure build-up and flow tests in wells, Dallas, 172 pp.

Ramey, H.J., JR (Editor), (1981): Reservoir engineering assessment of geothermal systems, Stanford Univ., Calif.

Riney, T.D. and Garg, S.K., (1982): Evaluation of injection test data from a Baca well. Proc. 8th Workshop Geothermal Reservoir Engineering, Stanford Univ., Calif. 97-100.

Rorabaugh, M.I., (1953): Graphical and theoretical analysis of step-drawdown tests of artesian well, Proc. Am. Soc. Engrs, 79, Separate No, 362, 23 pp.

Stefansson, V., Steingrimsson, B., (1981): Geothermal logging I, An Introduction to techniques and interpretation, 117 pp.

Stefansson, V., Steingrimsson, B., (1980b): Production characteristics of wells tapping two phase reservoirs at Krafla and Namafjall, Stanford, 6, 49-59.

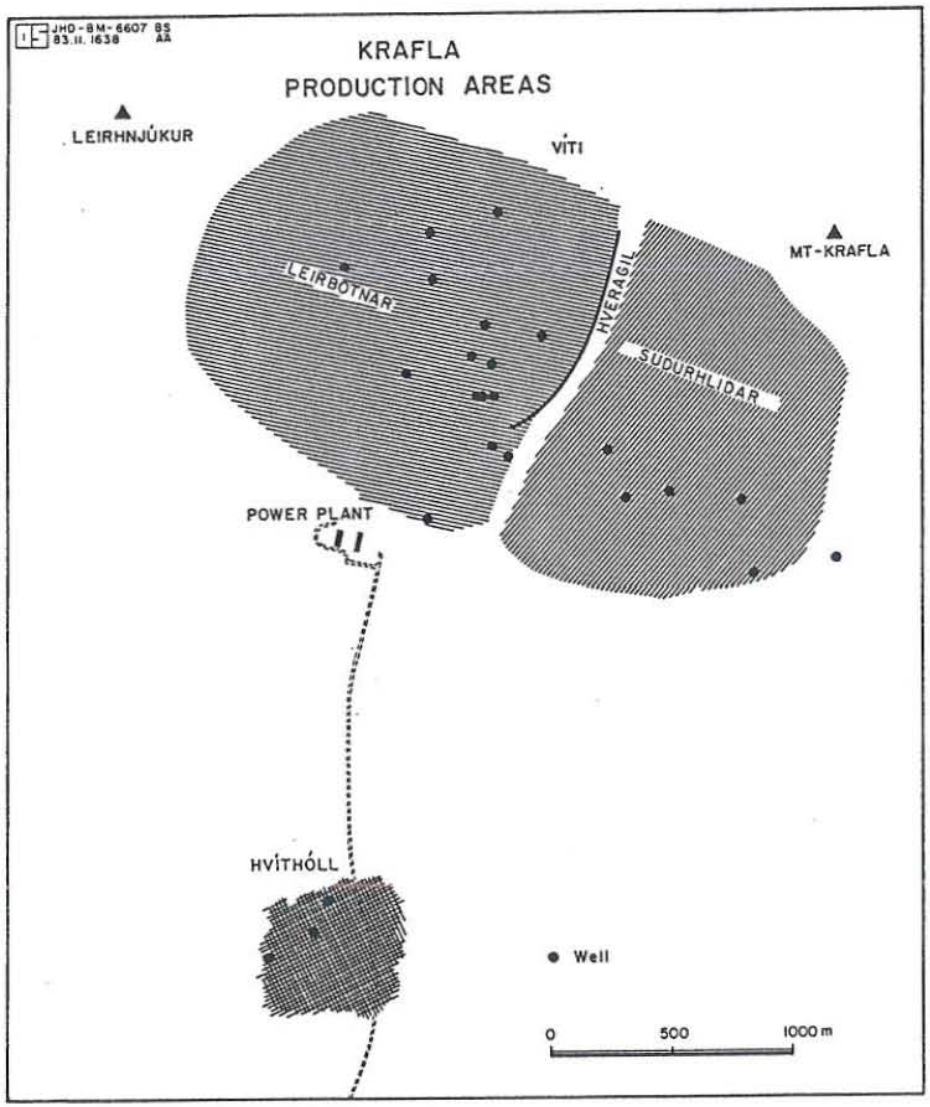

Fig. 1 Krafla production areas.

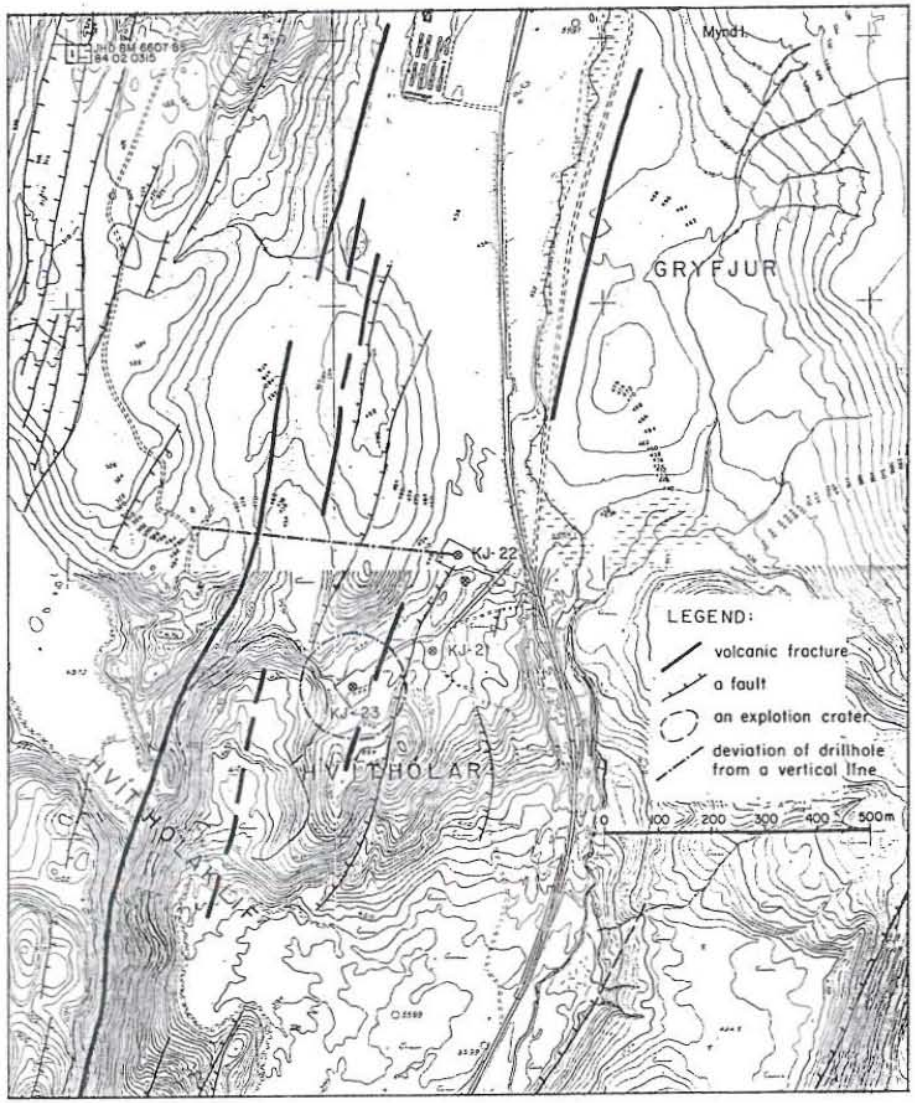

Fig. 2 General map of the Hvitholar geothermal area and location of wells.

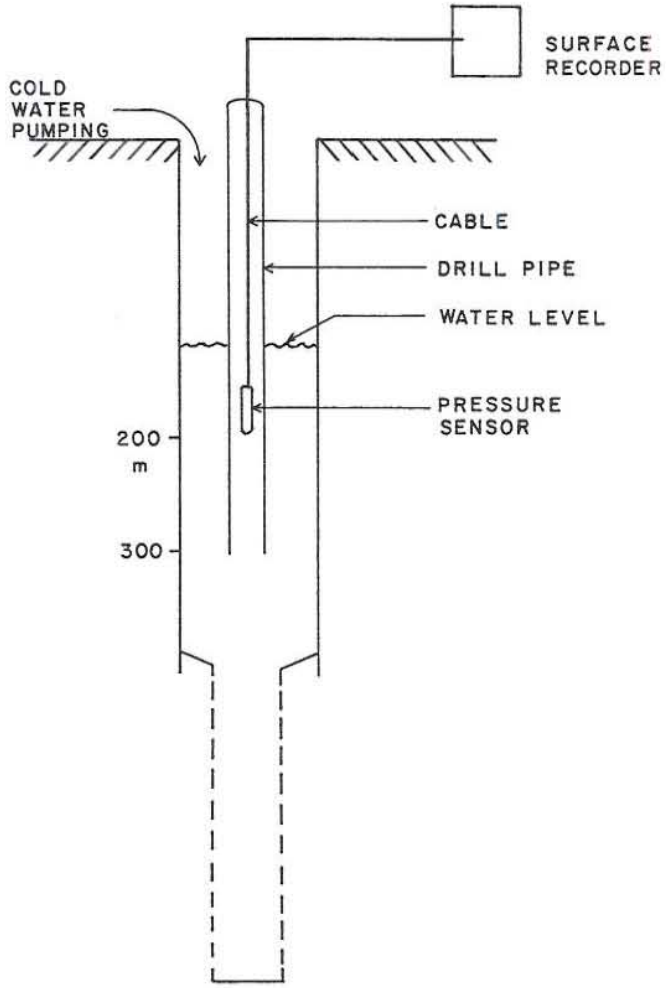

Fig. 3 Instrumental setup for injection test.

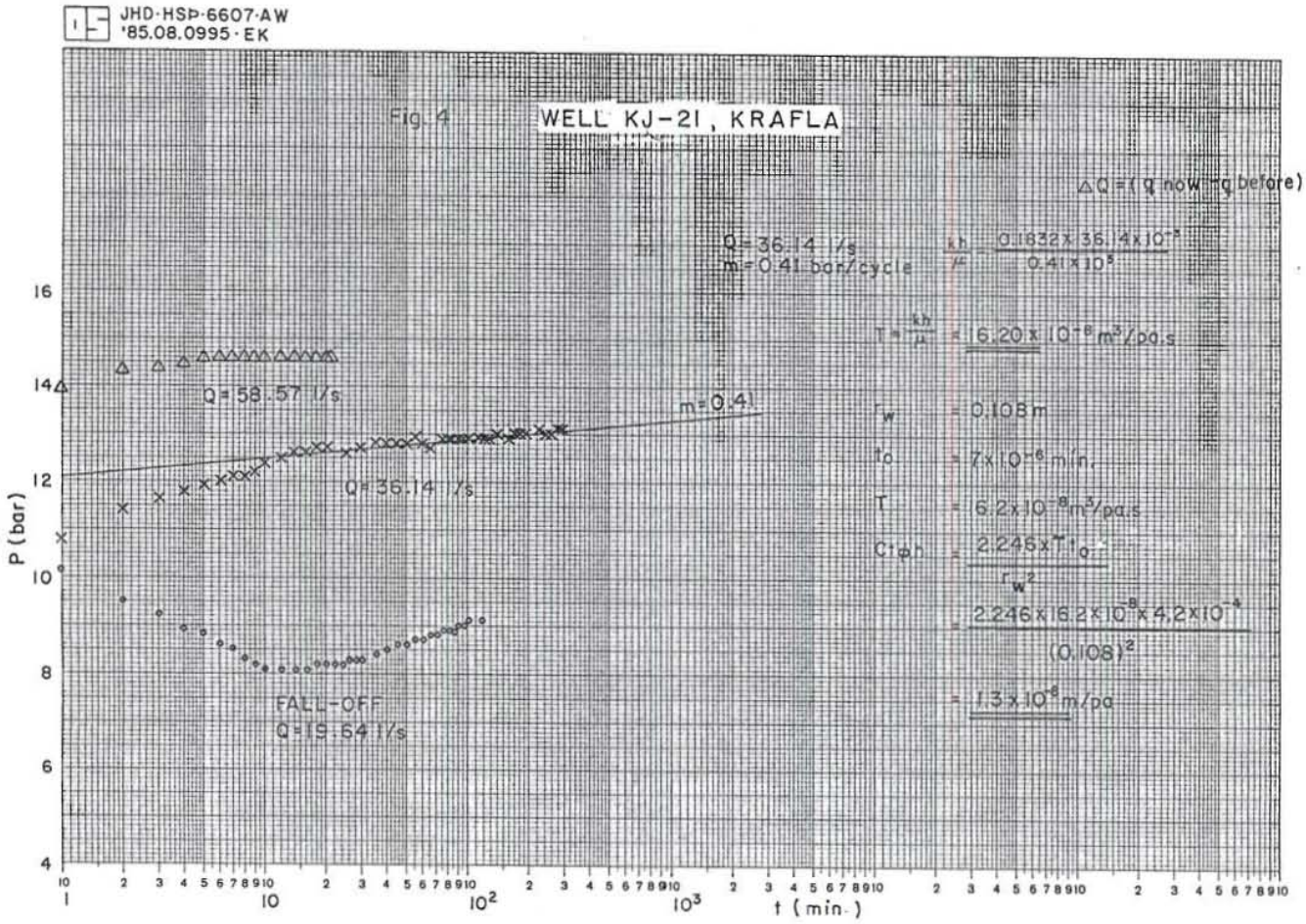

Fig. 4 Semilog plot of injection test data, well KJ-21.

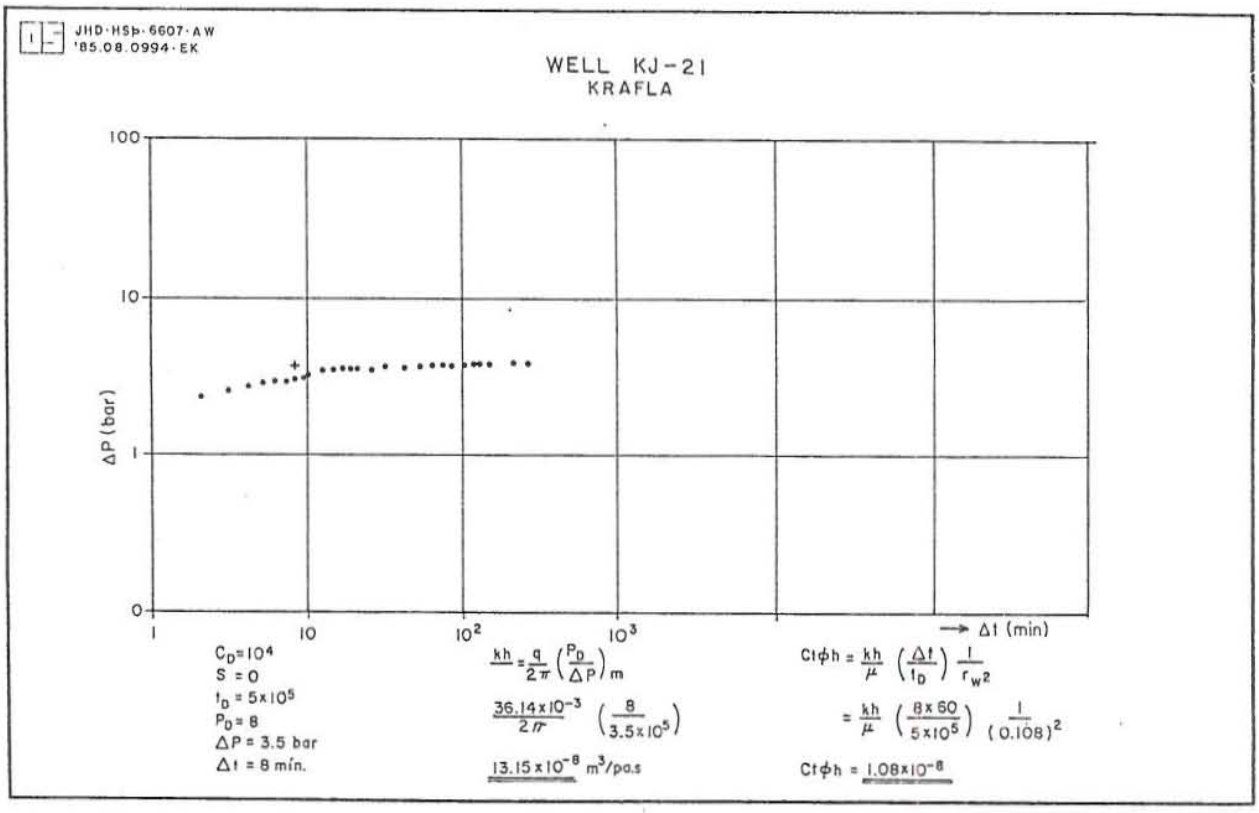

Fig. 5 Type-curve match for injection test data, well KJ-21.

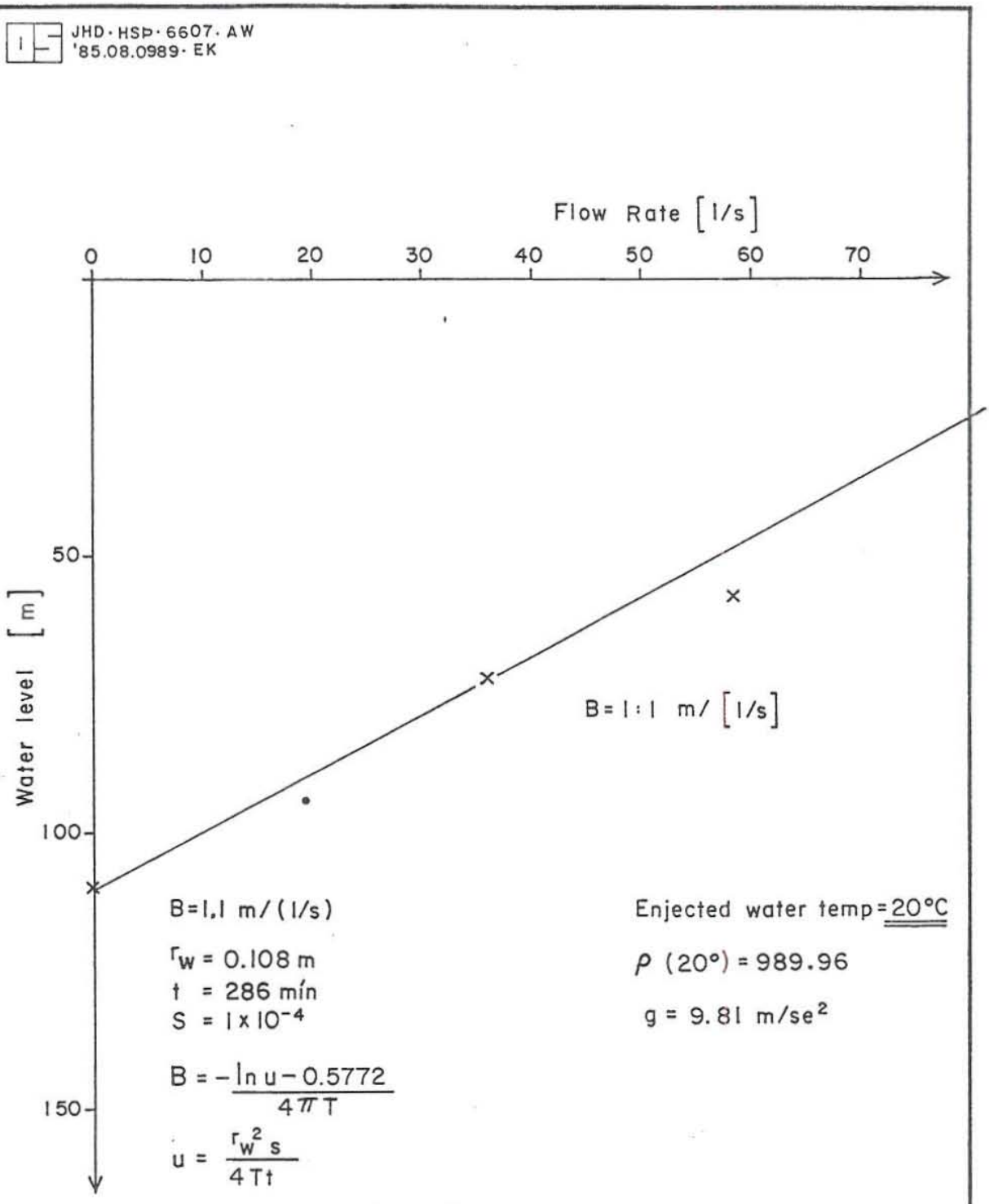

Fig. 6 Water level against flow rate plot for injection test data, well KJ-21.

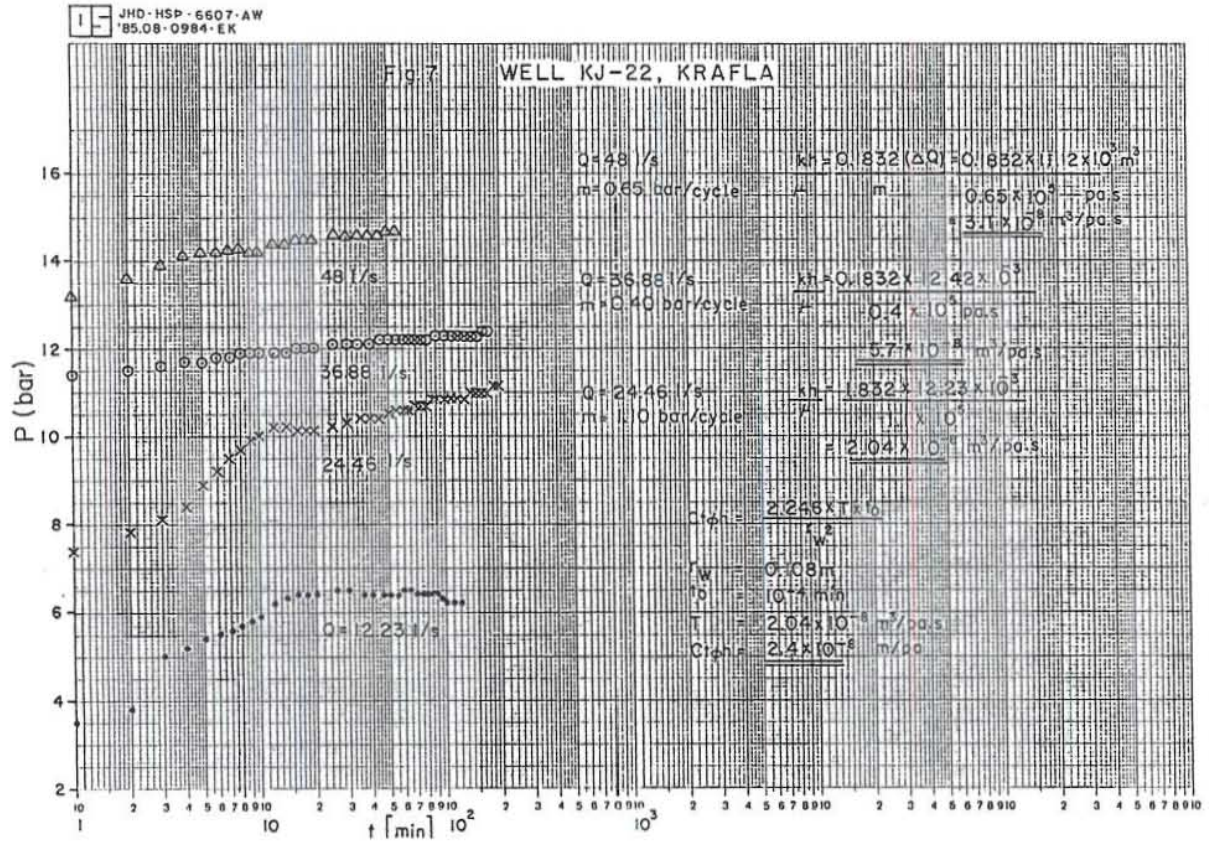

Fig. 7 Semilog plot of injection test data, well KJ-22.

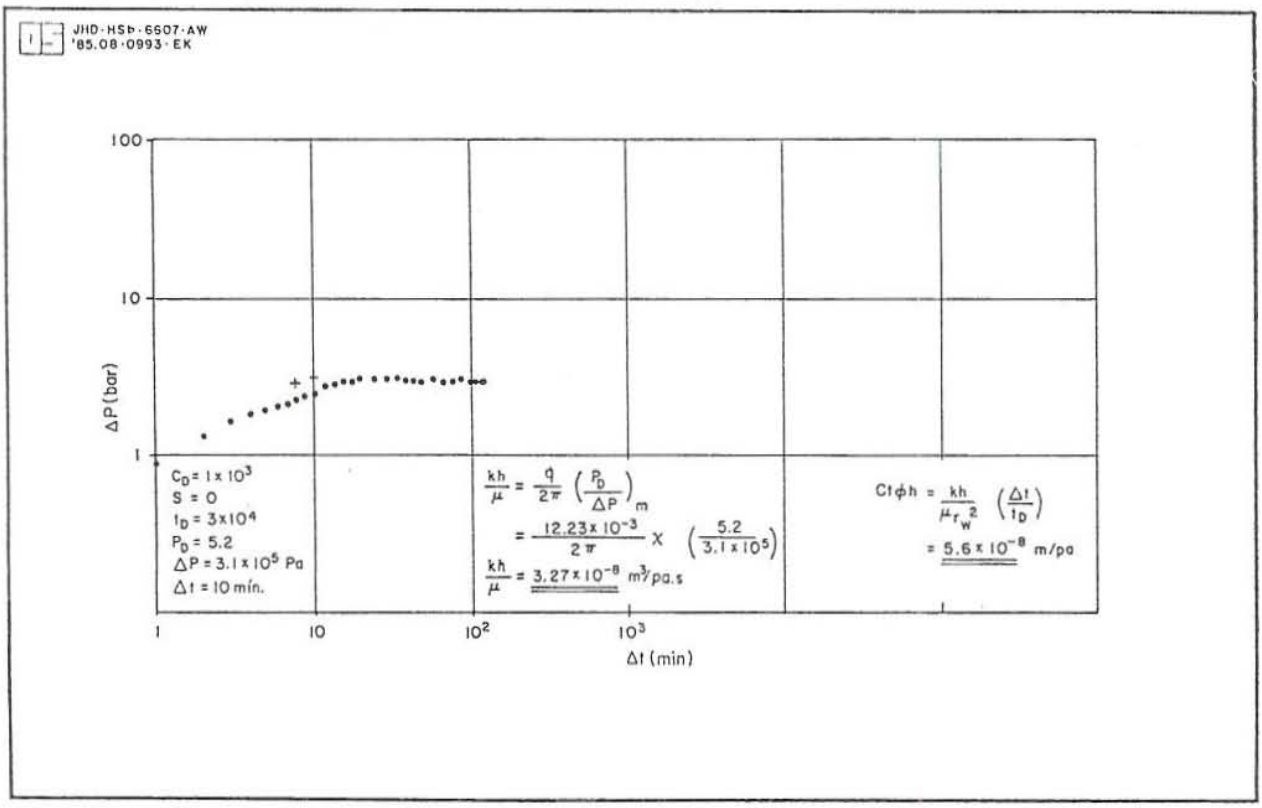

Fig. 8 Type curve match for injection test data for well KJ-22.

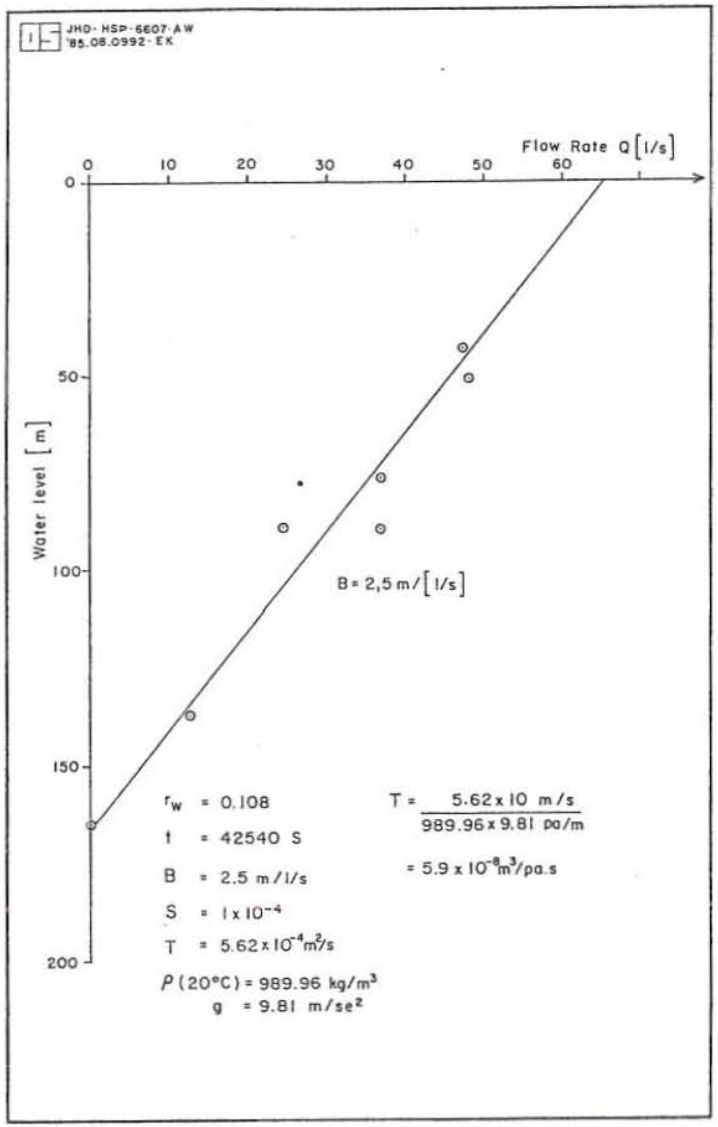

Fig. 9 Water level against flow rate plot for injection test data, well KJ-22.

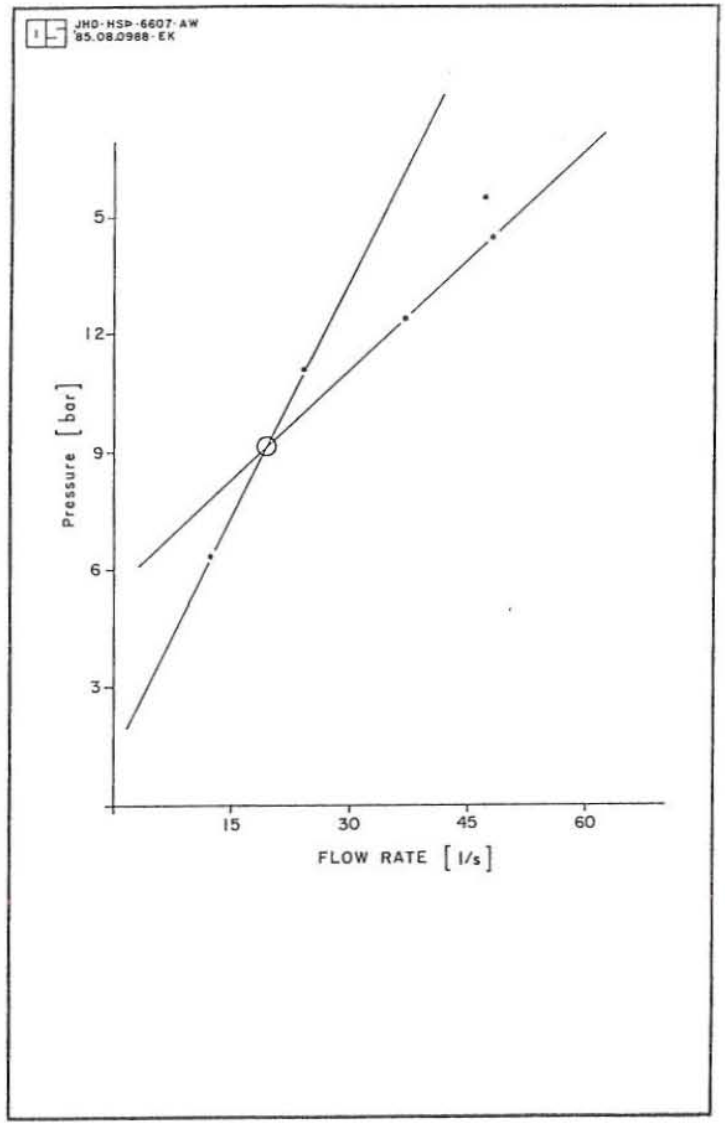

Fig. 10 Step rate injectivity plot for well KJ-22.

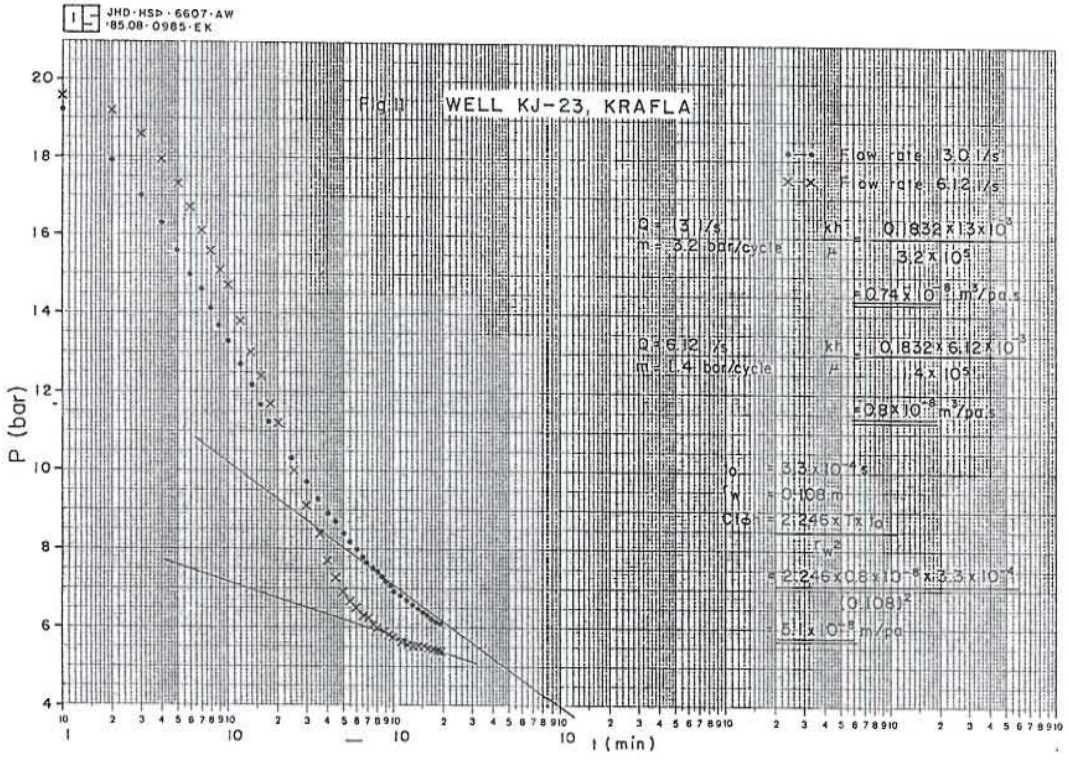

Fig. 11 Semilog plot of pressure fall-off, subsequent to injection of 6.12 l/s and 13 l/s for well KJ-23.

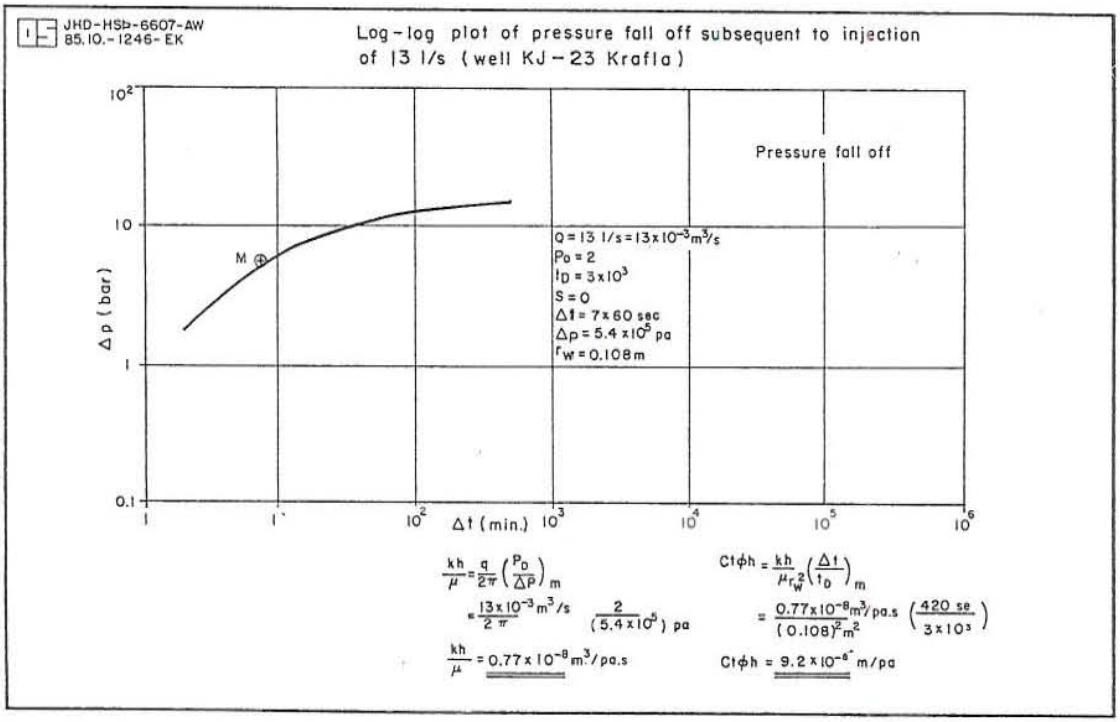

Fig. 12 Log-log plot for pressure fall-off subsequent to injection of 13 l/s for well KJ-23.

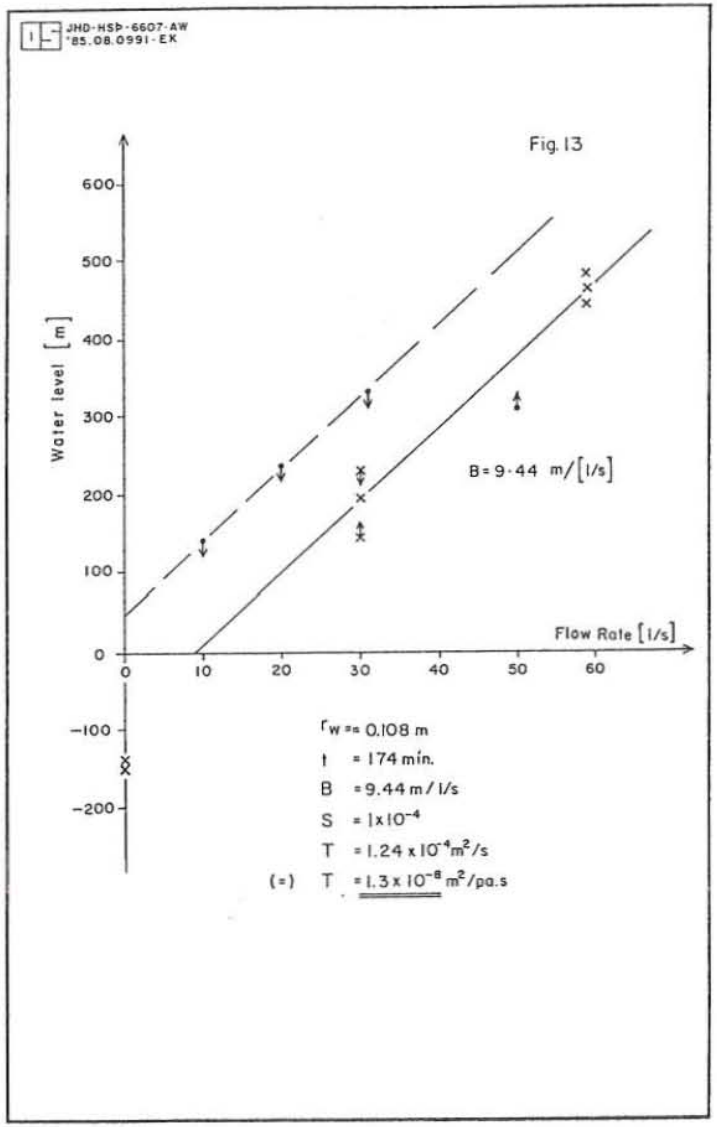

Fig. 13 Water level against flow rate plot for injection test data, well KJ-23.

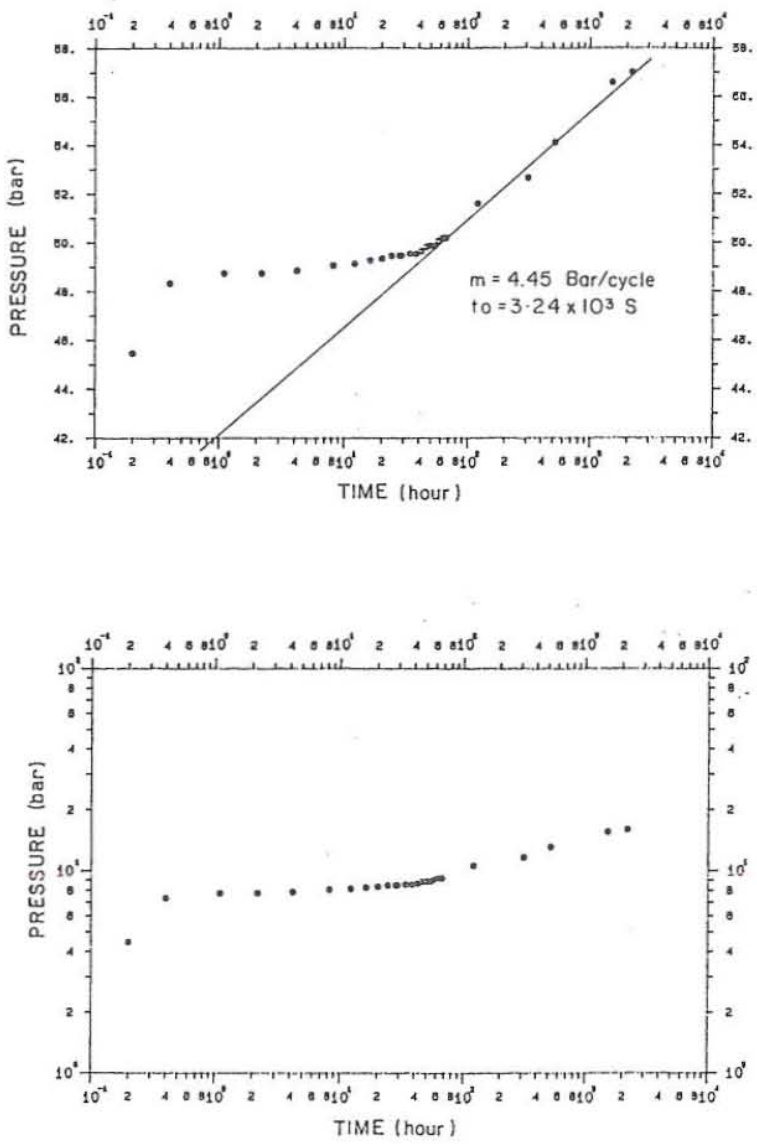

Fig. 14 Semilog plot for pressure build-up data, well KJ-21.

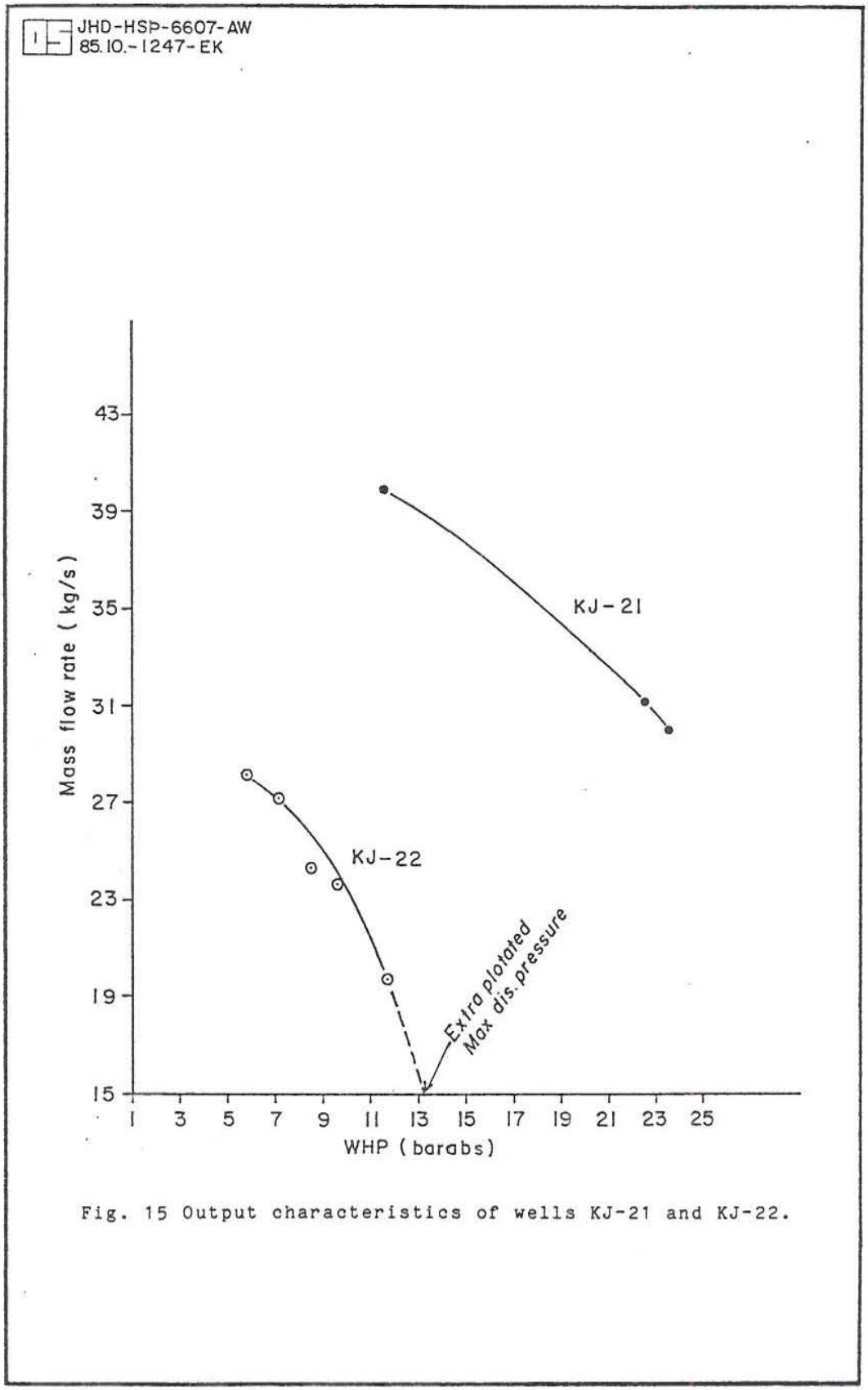

Fig. 15 Output characteristics of wells KJ-21 and KJ-22.

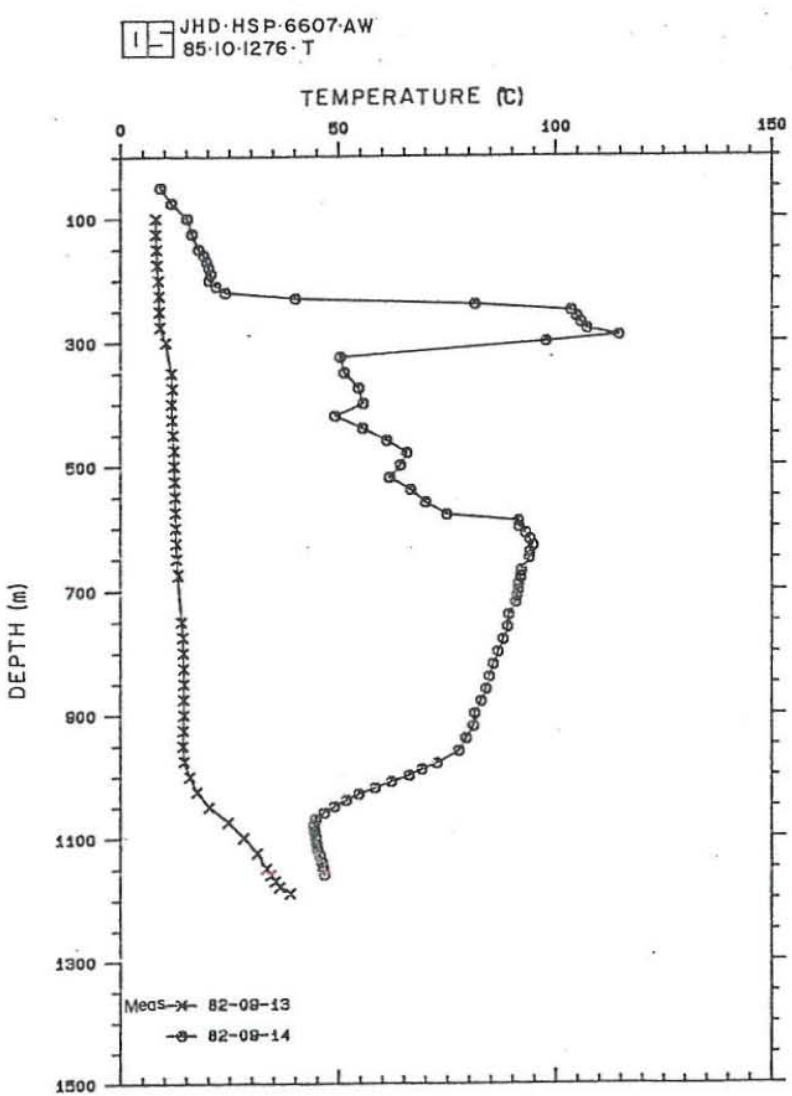

Fig. 16 Temperature profile during drilling, well KJ-21.

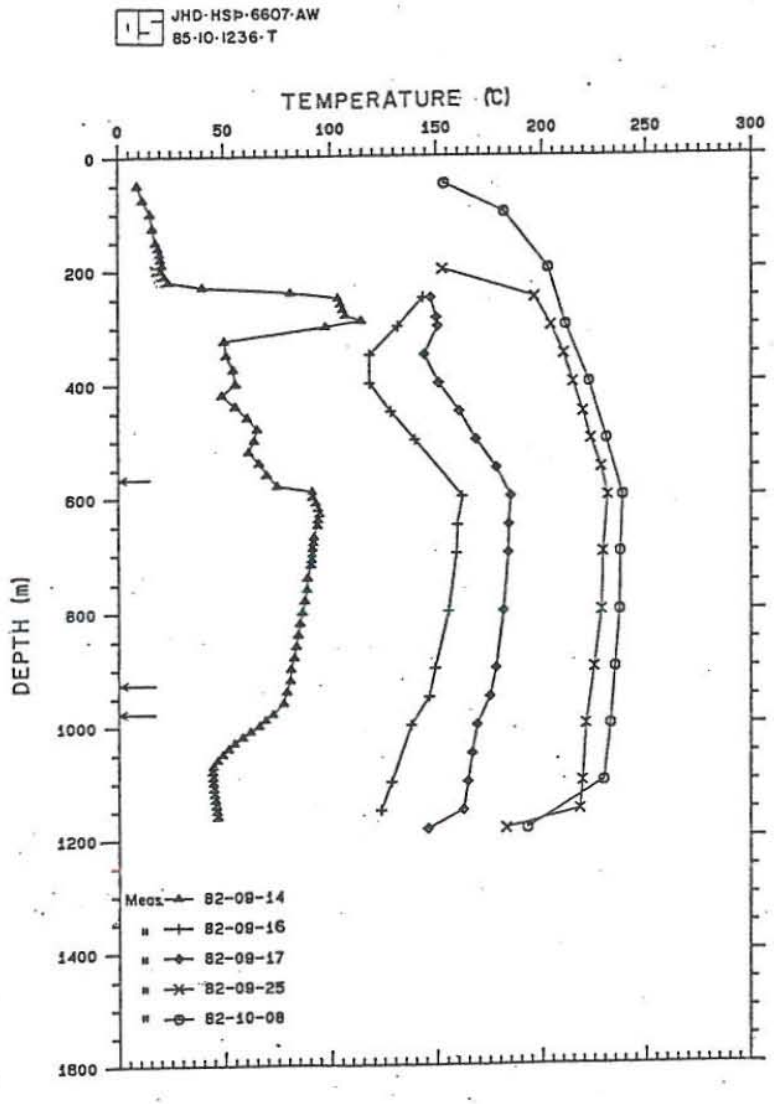

Fig. 17 Temperature profile during heating-up, well KJ-21.

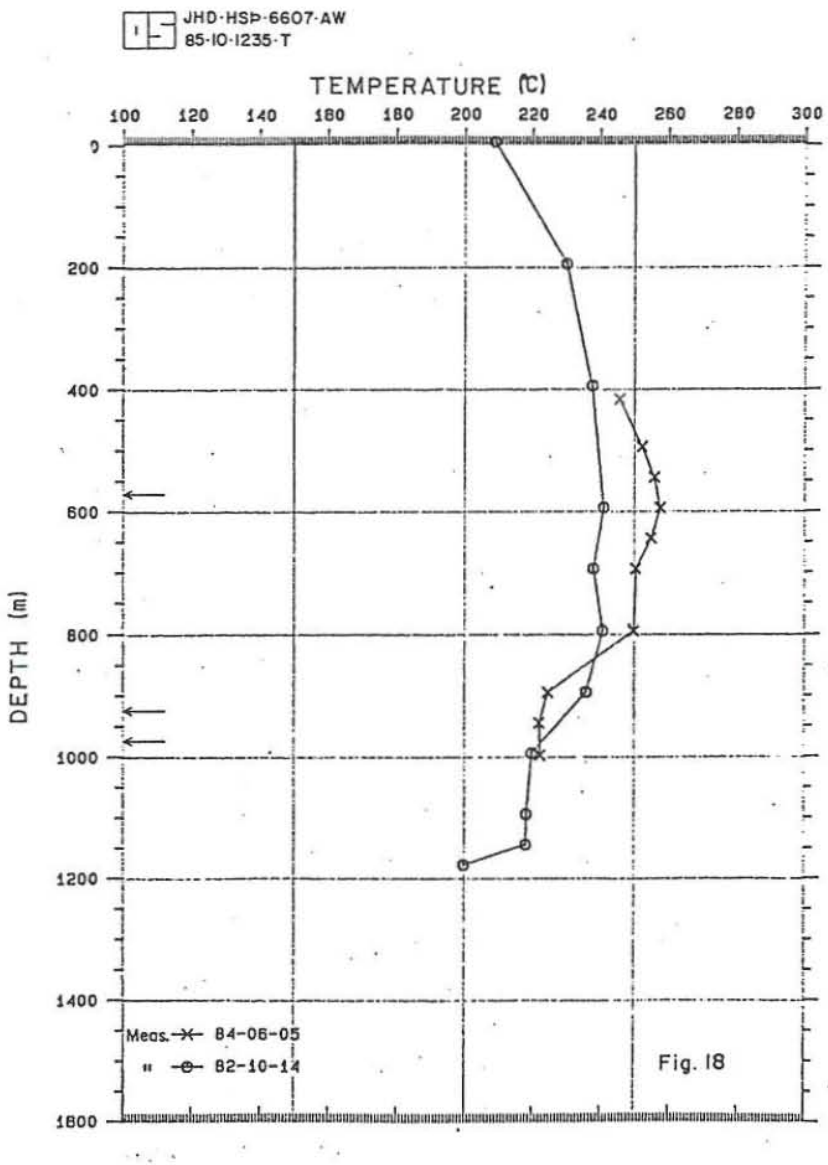

Fig. 18 Temperature profile after discharge, well KJ-21.

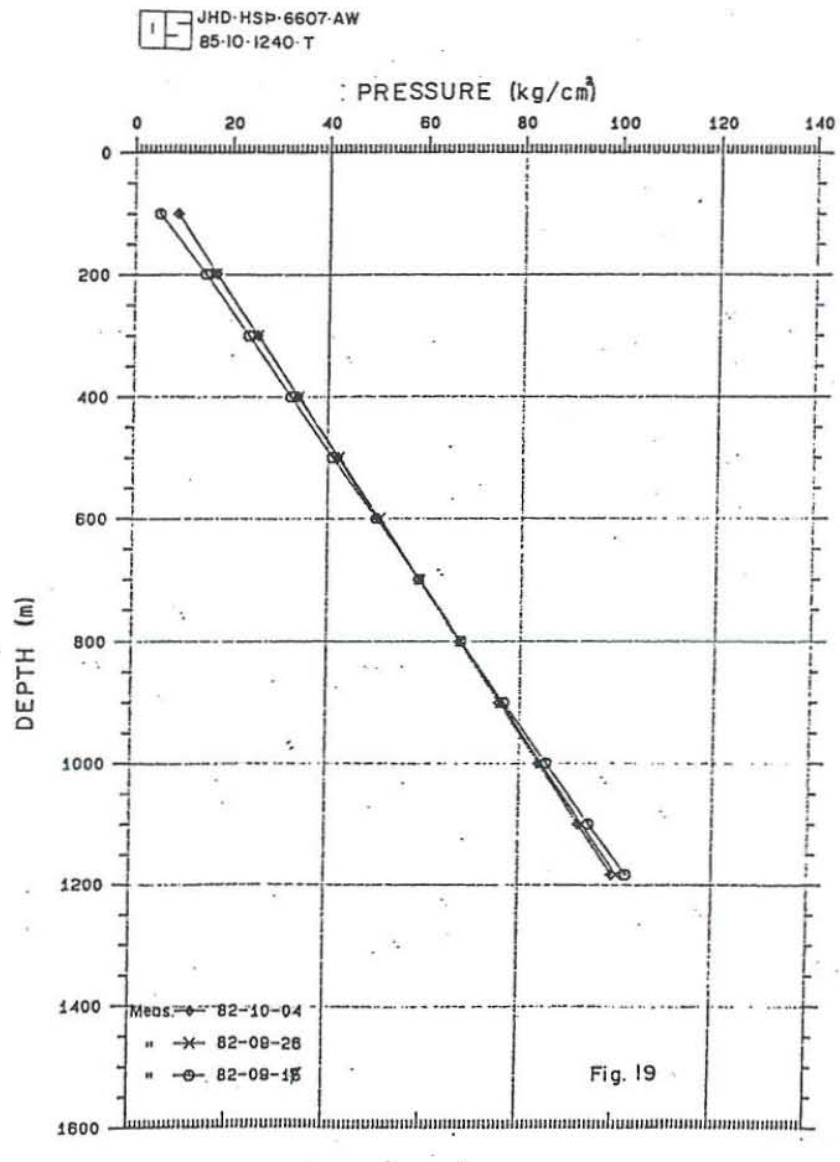

Fig. 19 Pressure profile in 1982, well KJ-21.

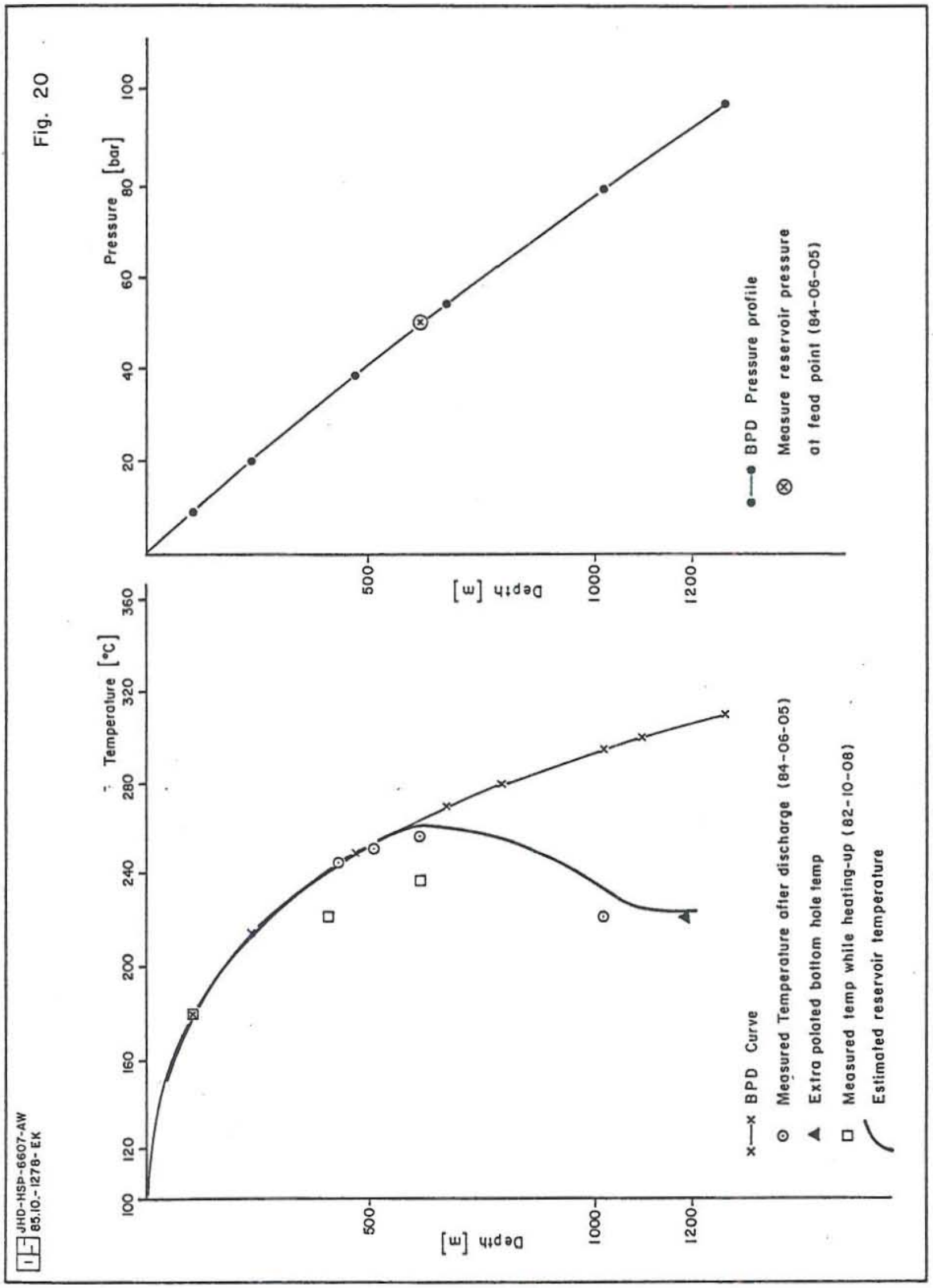

Fig. 20 Boiling point curves and reservoir temperature and pressure, well KJ-22.

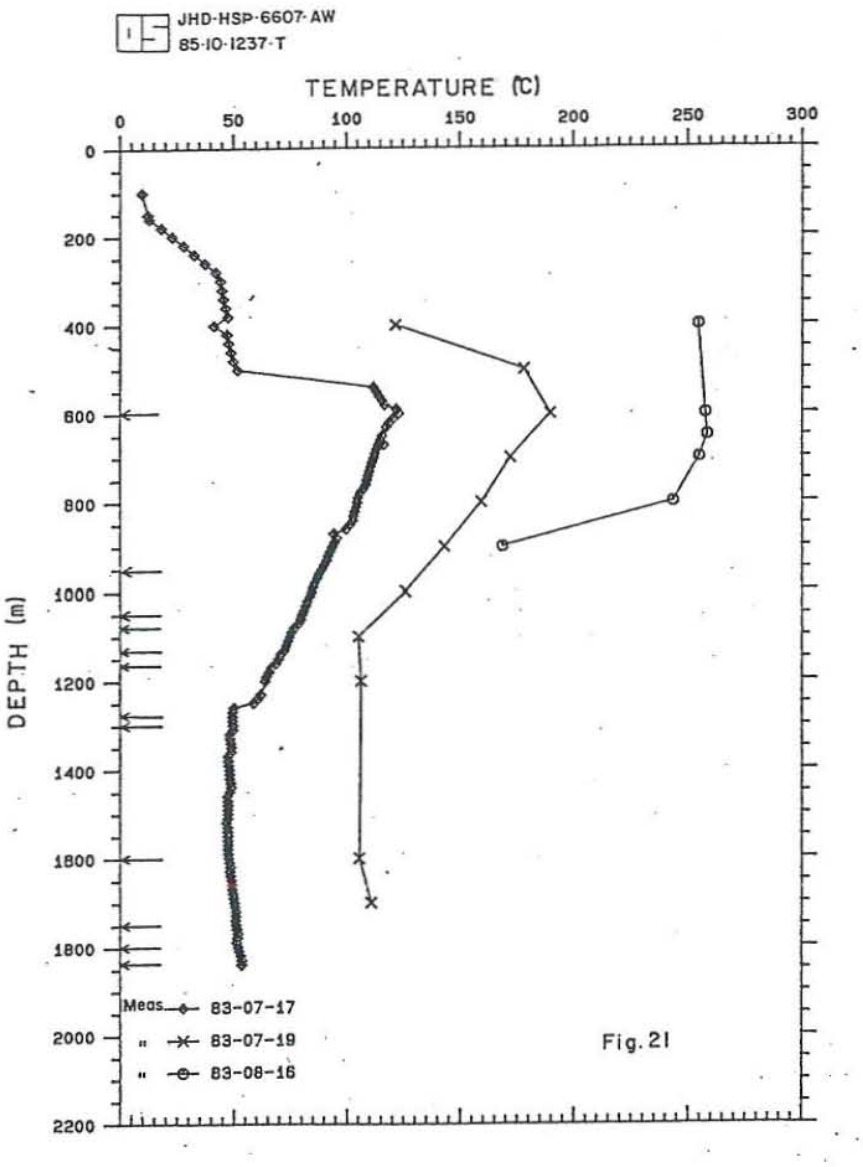

Fig. 21 Well KJ-22 temperature profile during heating-up.

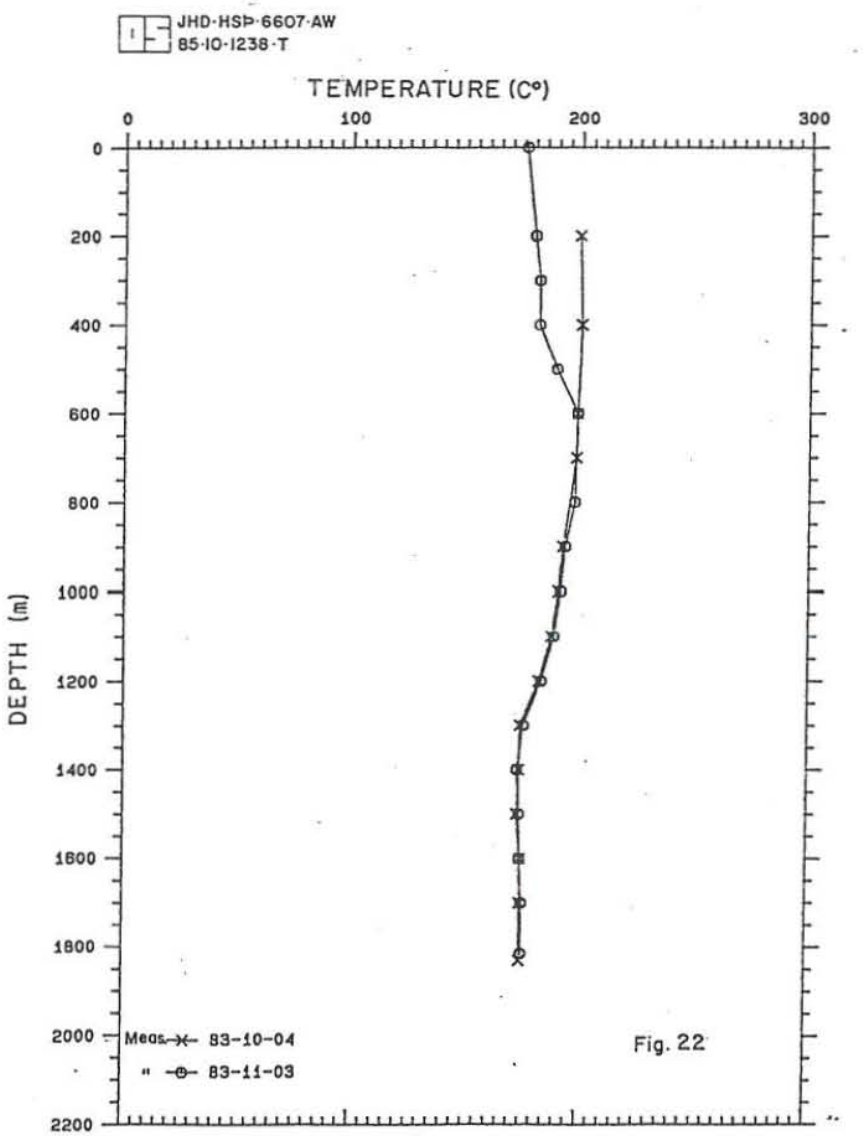

Fig. 22 Well KJ-22 temperature profile after discharge.

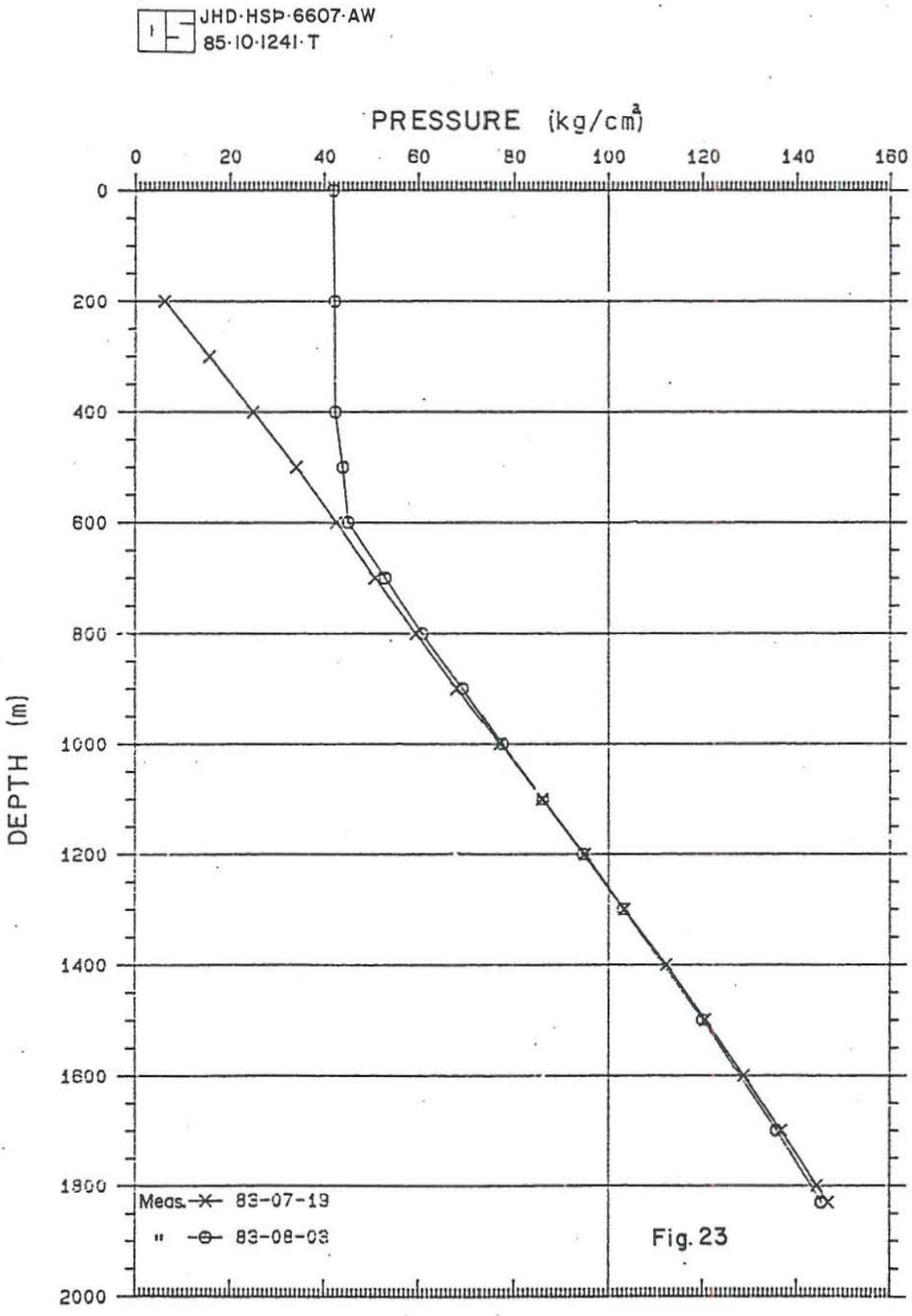

Fig. 23 Well KJ-22 pressure profile in 1983.

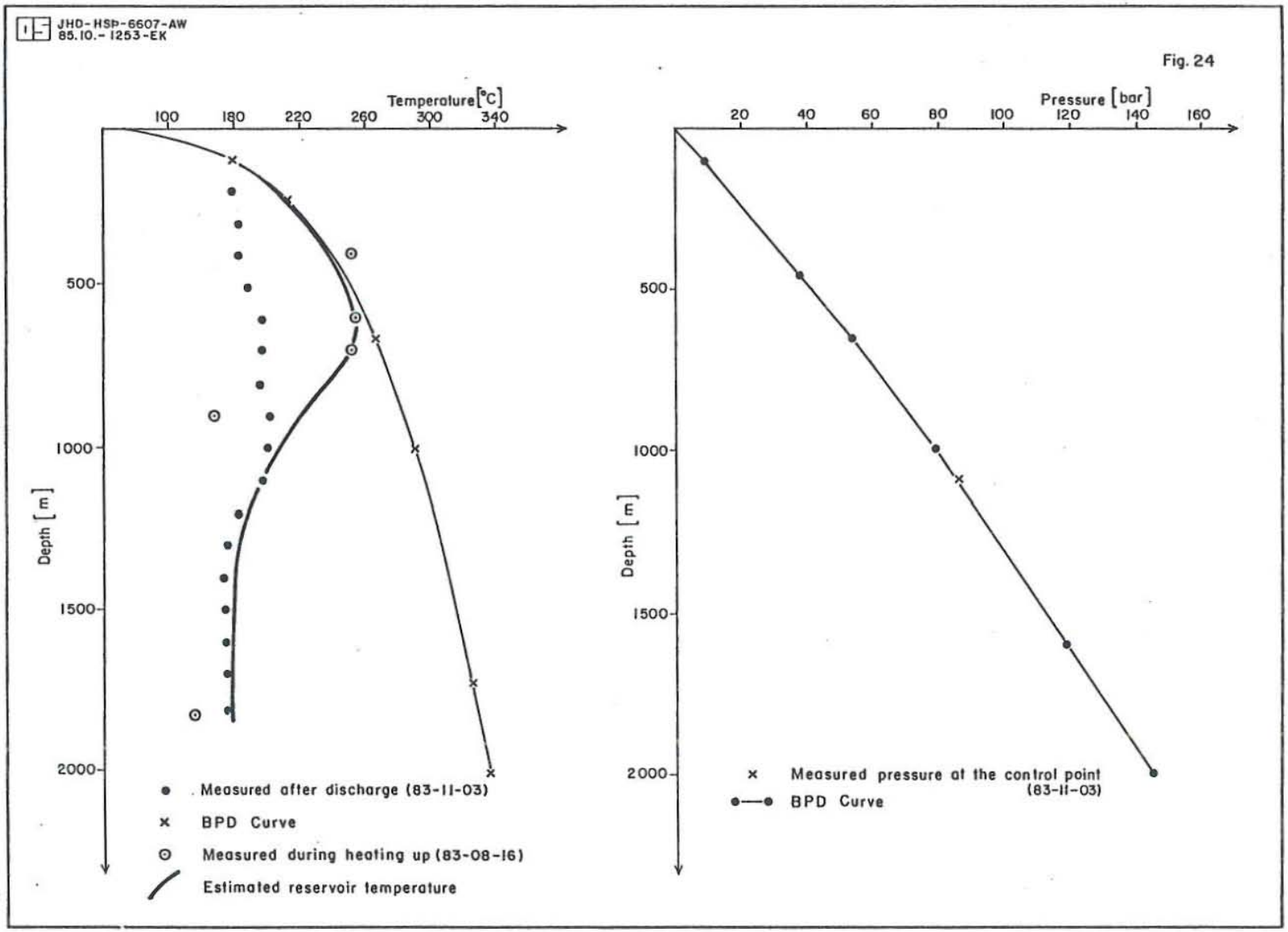

Fig. 24 Well KJ-22 reservoir temperature, pressure from logs and boiling point curves.

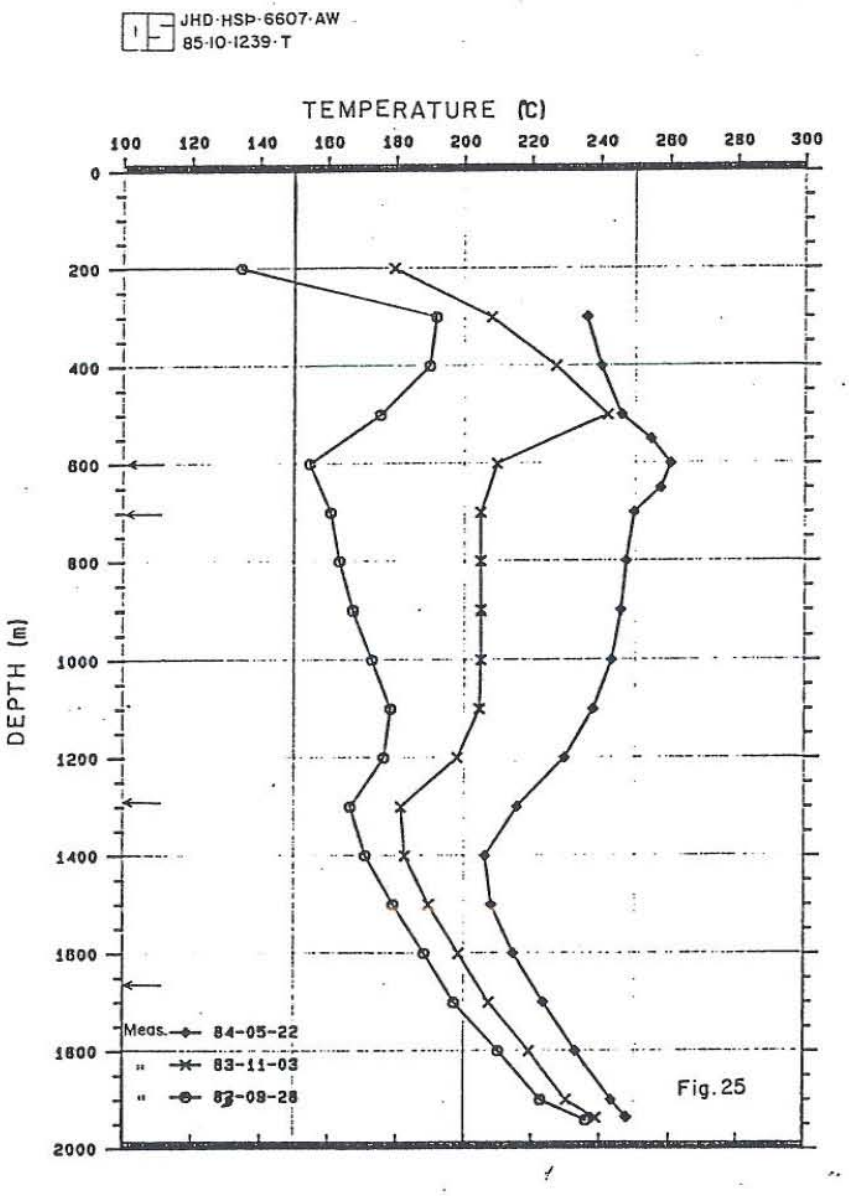

Fig. 25 Well KJ-23 temperature profile during heating-up.

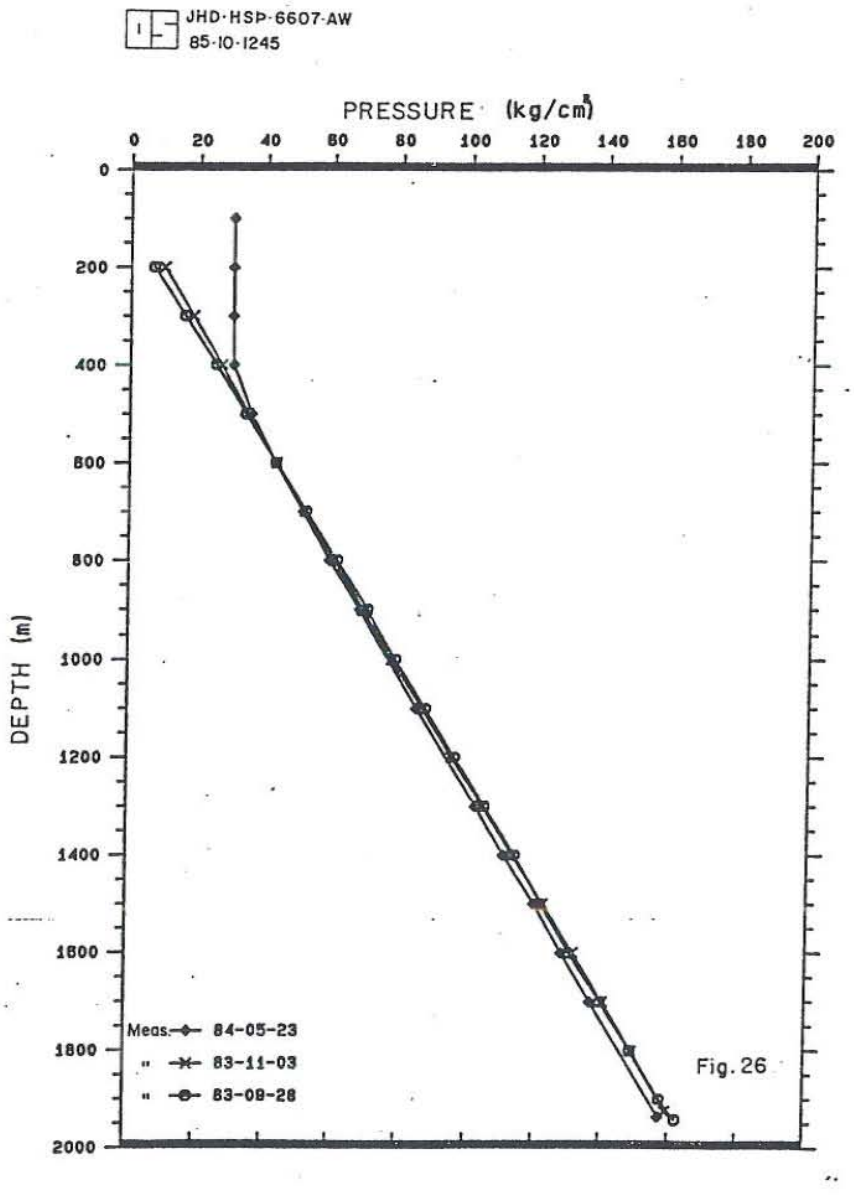

Fig. 26 Well KJ-23 pressure profile during heating-up.

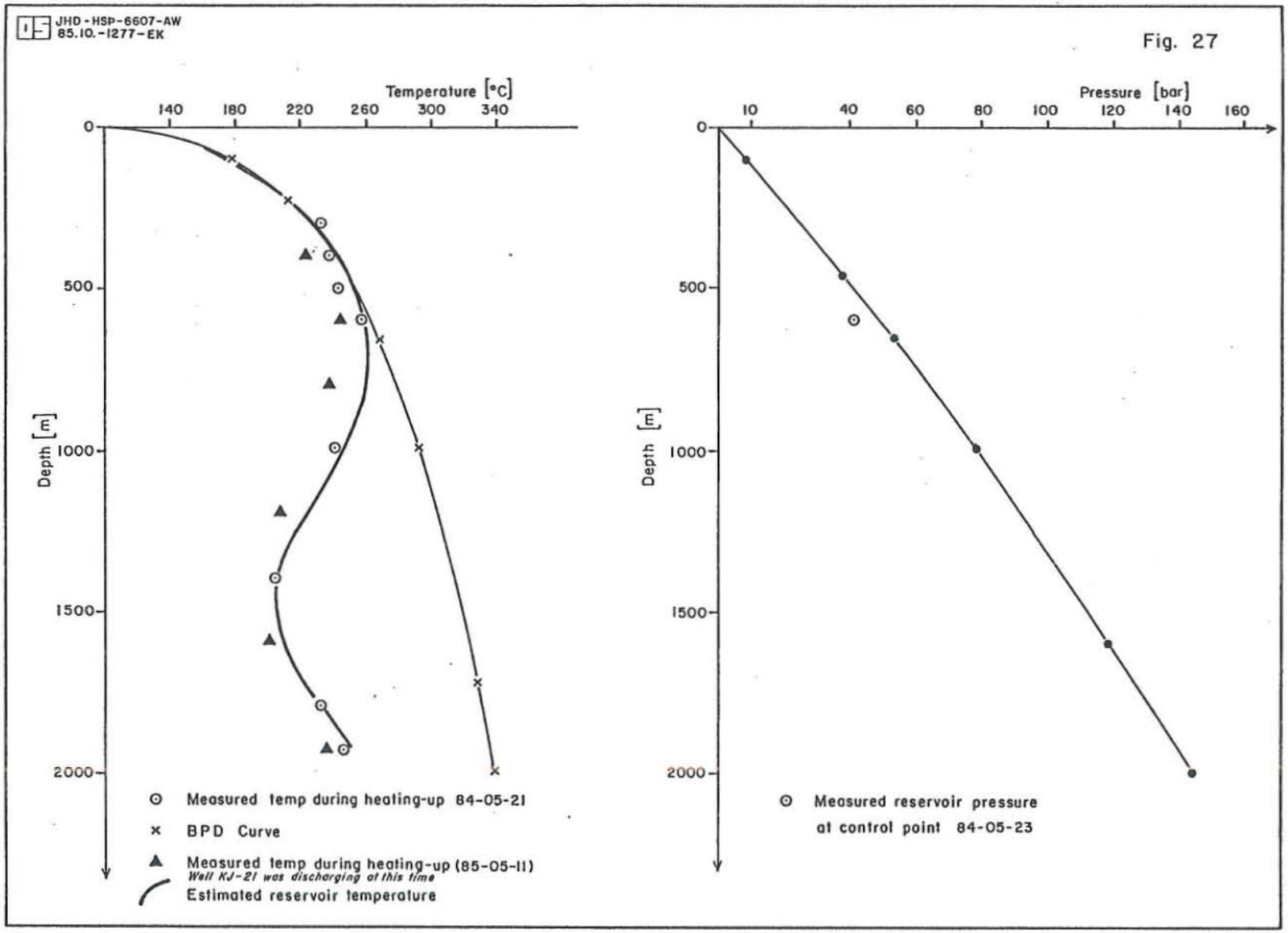

Fig. 27 Reservoir pressure and tempeature in relation to boiling point curves for well KJ-23.

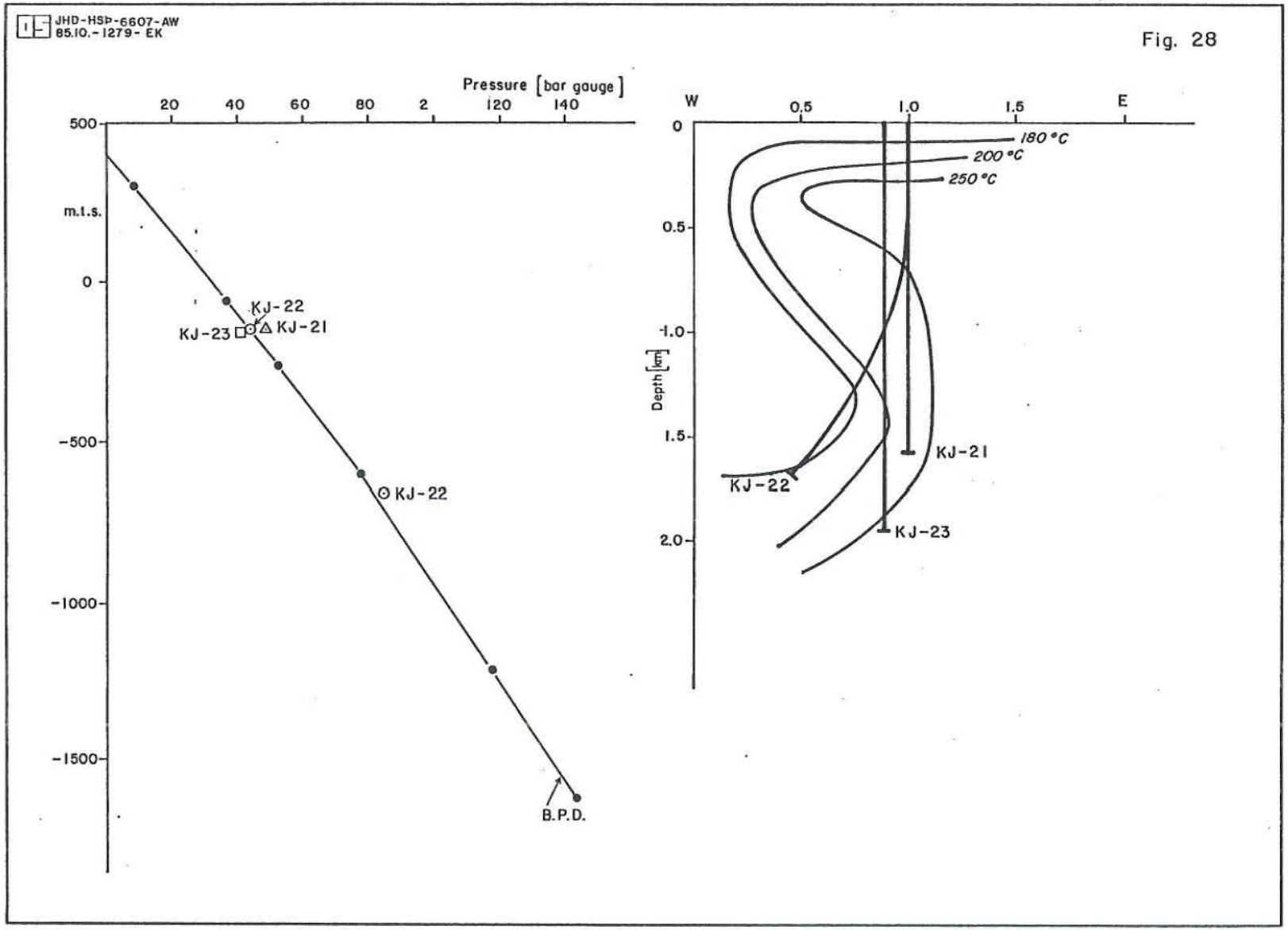

Fig. 28 Temperature distribution in an E-W cross section of the Hvitholar geothermal field, along with a reservoir pressure profile.